THERMODYNAMIC ANALYSIS OF INTERACTION OF CARBON WITH TiO_2, ZrO_2, AND B_2O_3 AND OBTAINING OF MIXTURE OF BORIDES AND CARBIDES OF TITANIUM AND ZIRCONIUM

J. I. Bagdavadze,[a] Z. N. Tsikaridze,[a] and K. Z. Ukleba[a]

Keywords: thermodynamic analysis; synthesis; composite materials; carbon; titanium dioxide; zirconium dioxide; boron oxide

Metal borides and carbides, TiB_2/TiC and ZrB_2/ZrC are widely used nanostructured composite materials. A detailed thermodynamic analysis was performed to determine the formation conditions of titanium and zirconium borides and carbides in the Ti–B–O–C and Zr–B–O–C systems. The complete thermodynamic analysis was carried out in vacuum for the reactions $2TiO_2 + B_2O_3 + 8C = TiB_2 + TiC + 7CO$ and $2ZrO_2 + B_2O_3 + 8C = ZrB_2 + ZrC + 7CO$. On the basis of the theoretically found results, experimental synthetic routes were developed to prepare TiB_2/TiC and ZrB_2/ZrC composite materials.

* Corresponding Authors
E-Mail: ketino.ukleba@gmail.com
[a] Ferdinand Tavadze Metallurgy & Materials Science Institute, Laboratory of Boron & Composite Materials, 10 Elizbar Mindeli Street, Tbilisi, 0160 Georgia

INTRODUCTION

The nanostructured composite materials, including metal borides and carbides containing ones like TiB_2/TiC and ZrB_2/ZrChave a unique set of physical and chemical properties (high hardness, heat resistance, high-temperature strength, electrical and thermal conductivities, and resistance to the molten metals in combination with low specific weight, corrosion-, radiation- and wear-resistance).

There are some known methods to obtain of these composites,[1–7] but a complete thermodynamical analysis[8] of the system to optimize their synthesis conditions have not been performed yet. In this work, the comprehensive thermodynamical analysis has been conducted to find optimal conditions for preparation of carbides and borides of zirconium and titanium.

EXPERIMENTALS

Computer calculations were carried out with the ASTRA–4 program described in [8]in the temperature range 500–2000K with the step of 50K for vacuum conditions. The mixture of ZrB_2–ZrC was prepared by mixing the powders of ZrO_2, B_2O_3 and C followed by 30h grinding in a high power (1000rpm) mill. The mill was a piece of special equipment designed and built in our laboratory. After briquetting, the obtained powder was sintered in a high vacuum oven under an argon atmosphere at ~1400°C for 5 h.

RESULTS AND DISCUSSION

System Ti–B–O–C

The thermodynamical analysis of Ti–B–O–C system in vacuum is carried out for the reaction:

$$2TiO_2+B_2O_3+8C=TiB_2+TiC+7CO \qquad (1)$$

The following species were considered as possible condensed and gaseous components: C, Ti, TiO, Ti_2O_3, TiO_2, Ti_3O_5, Ti_4O_7, TiC, $TiCO_{0.04}$, $TiC_{0.10}O$, $TiC_{0.40}O_{0.60}$, $TiC_{0.75}O_{0.25}$, B, B_2O_3, B_4C, TiB, TiB_2, and Ar, O, O_2, O_3, C, C_2, C_3, C_4, C_5, CO, CO_2, C_2O, C_3O_2, Ti, TiO, TiO_2, B, B_2, BO, BO_2, B_2O, B_2O_2, $B_2O_3$and TiB,.

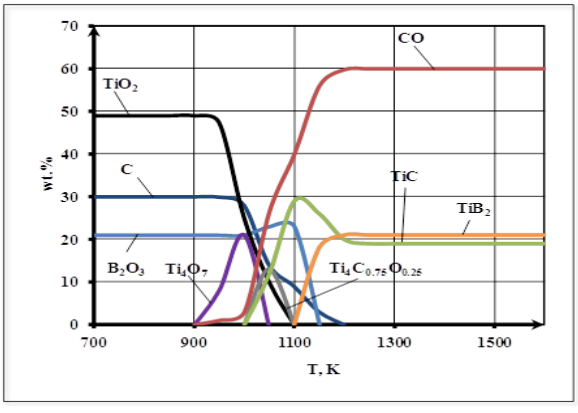

Figure 1. Dependence of components content on temperature for reaction (1) in vacuum (0.0001 atm) in temperature interval 700–1600 K.

The knowledge of reliable thermodynamic data of the reactive system components is necessary. Since some thermodynamic characteristics (ΔH_{298}, $T_{m.}$, $\Delta H_{m.}$, C_p, and

$C_{p(L)}$) of the abovementioned oxycarbides cannot be obtained from the literature, the corresponding thermodynamic constants of oxycarbides were calculated.[9]

The main results of the thermodynamic calculations for the Ti–B–O–C system are presented in Figure 1. It is evident that the reduction of TiO_2 begins above 900 K, and Ti_2O_3, Ti_3O_5 and Ti_4O_7 are allocated in the condensed phase. Their amounts increase to ~1000 K, but raising the temperature their amount started to decrease, and at~1100 K all of the titanium oxides disappear entirely. It appears some amount of condensed carbon and simultaneous allocation of CO in the gas phase begin at temperatures higher than 900K. At ~1200 K, the condensed carbon disappears and the amount of CO reaches its maximum which does not change further. At ~1000 K appears the allocation of TiC which amount sharply increases to ~1100 K and reaches its maximum (~29 wt. %). Increasing the temperature, its amount decreases to ~1200 K and its amount (~18 wt.%) does not change until 1600 K.

The thermodynamic analysis showed that the experiments have to be conducted in vacuum at temperatures higher than 1200K to obtain the requested TiB_2–TiC mixtures.

The system Zr–B–O–C

The detailed thermodynamic analysis of the Zr–B–O–C system in vacuum was carried out for the reaction:

$$2ZrO_2+B_2O_3+8C=ZrB_2+ZrC+7CO. \quad (2)$$

As possible condensed and gaseous components the following ones were considered: C, B, B_2O_3, B_4C, Zr, ZrO_2, ZrC, ZrB_2, and Ar, O, O_2, O_3, B, B_2, BO, BO_2, B_2O, B_2O_3, C, C_2, C_3, C_4, C_5, CO, CO_2, C_2O, C_3O_2, Zr, Zr_2, ZrO, ZrO_2, respectively.

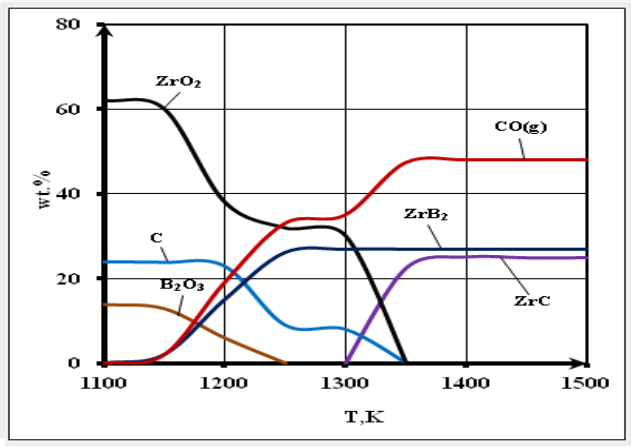

Figure 2. Dependence of components content on temperature for reaction (2) in vacuum (0.0001 atm) in temperature interval 1100–1500 K.

The results of the thermodynamical analysis performed on the Zr–B–O–C system are presented in Figure 2. A reduction process occurs above ~1100 K with the formation of zirconium diboride ZrB_2. Its amount increases up to ~1250K where reaches its maximum (~27 wt.%) and above this temperature does not change further. The amounts of condensed B_2O_3 and ZrO_2 were sharply decreased above~1100 K and completely disappeared at ~1250 and ~1350 K, respectively.

The condensed carbon amount smoothly changes around ~1100 K, but above this temperature its amount sharply decreases and completely disappears at ~1350 K.The condensed zirconium carbide ZrC is allocated above 1300 K, its amount drastically increases up to ~1350K reaching 25 wt.%, but above this temperature there are no further changes in its amount. Thermodynamic analysis of reaction 2 showed that the experiments should do above 1350 K.in vacuum to obtain the expected ZrB_2 and ZrC,

RESULTS

Based on the results of thermodynamic calculations, some tests have been done to prepare TiB_2–TiC mixtures from the mixture of TiO_2 and B_2O_3 with C (graphite) or with ZrO_2-B_2O_3/graphite mixtures in a high-temperature furnace in the argon atmosphere at ~1400°C for 3h.The X-ray diffraction patterns of the prepared powder are given in Figure 3.

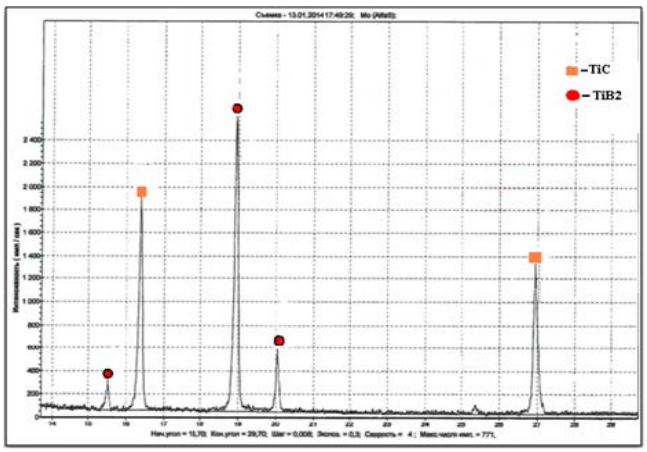

Figure 3. The X-ray diffraction pattern of a mixture of TiB_2 and TiC prepared from TiO_2-B_2O_3/graphite mixture at 1400 °C in 3 h

As can be seen, the product is ca. 1:1 mixture of TiB_2 and TiC.

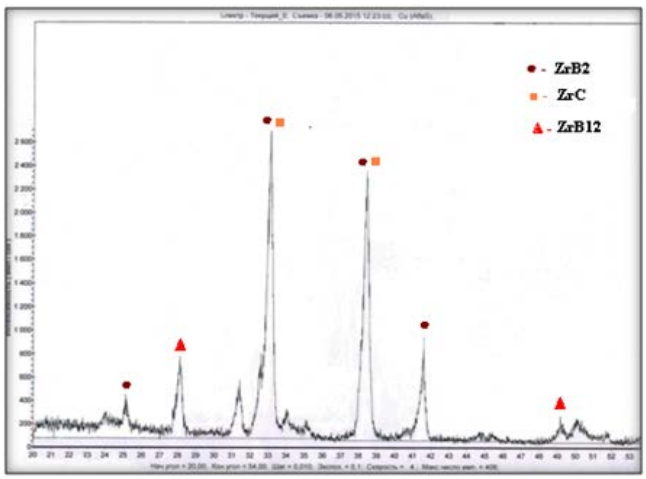

Figure 4. The x-ray diffraction pattern of a mixture of ZrB_2 and ZrC prepared from ZrO_2-B_2O_3/graphite mixture at 1400 °C in 3 h

ACKNOWLEDGMENT

Paper was presented at the 5th International Conference "Nanotechnologies", November 19–22, 2018, Tbilisi, Georgia (Nano–2018).

REFERENCES

[1]Zou, B., Huang, Ch., Song, J., Liu, Z., Liu, L., Zhao, Y., Effects of sintering processes on mechanical properties and microstructure of TiB_2–TiC + 8wt.% nano-Ni composite ceramic cutting tool material, *Mater. Sci. Eng. A*, **2012**, *540*, 235-244. DOI: 10.1016/j.msea.2012.02.002

[2]Kravchenko, S., Torbov, V., Shilkin. S., Receiving nano-dimensional powder of a diboride of the titanium. *Inorg. Mater.*,**2010**, *46(6)*, 691-693.

[3]Kim, J. W., Shim, J.H., Ahn, J. P., Cho, Y. W., Kim, J.-H., Mechanochemical synthesis and characterization of TiB_2 and VB_2 nano-powders. *Mater. Lett.*, **2008**, *62*, 16, 2461-2464.

4. Volkova, L. Kravchenko, S. Korobov, I. Kolesnikova, A. Dremova, N. Bulgakova, A. Kalinikov, G. Shilkin. S., Features of receiving nano-dimensional powder of a diboride of the titanium of various dispersions. *Inorg. Mater.*, **2013**, *49(11)*, 1173-1177.

[5]Ran, S., van der Biest, O., Vleugels, J., ZrB_2 powders synthesis by borothermal reduction. *J. Am. Ceram. Soc.*,**2010**, *93(6)*, 1586-1590. DOI: 10.1111/j.1551-2916.2010.03747.x.

[6]Guo, Sh., Hu, Ch., Kagawa, Y., Mechanochemical processing of nanocrystalline zirconium diboride powder. *J. Am. Ceram. Soc.*,**2011**, *94(11)*, 3643-3647.https://doi.org/10.1111/j.1551-2916.2011.04825.x

[7]Kiparisov, S-. Leninski, I., Petrov, A., *Titanium Carbide: Receiving, Properties, and Applications*, Moscow, Metallurgiya, **1987**, 216 pp.

[8]Vatolin, N. Moiseev, G. Trusov,B., *Thermodynamic Modeling in High-TemperatureInorganic Systems*, **1994**, Moscow, Metallurgiya, 352 pp.

[9]Gvelesiani, G. Bagdavadze. J., *Calculation Methods of Determination of ThermodynamicFunctions of Inorganic Substances and Their Application in Full Thermodynamic Analysis of Metallurgical Processes*, Tbilisi, Universal, **2006**, 127 pp.

Received: 06.01.2019.
Accepted: 26.02.2019.

KINETICS AND THERMODYNAMICS OF THE CORROSION OF MILD STEEL IN THE PRESENCE OF *EUPHOBIA TIRUCALLI* GUMS

Habibat Faith Chahul[a]*Elijah Maji[a] and Rufus Shaato[a]

Keywords:*Euphobia tirucalli*, adsorption isotherm, activation energy, corrosion inhibition

Understanding the mechanism of corrosion of steel in acidic environments along with the accompanying quest for corrosion inhibitors that are nontoxic to the environment is of significant industrial concern. This work sets to investigate the corrosion of mild steel in 1.0 M solution of HCl in the presence of *Euphobia tirucalli* gums (ET) using weight loss and linear polarization measurements. The study was carried out within the inhibitor concentration range of 0.2-1.0 g L^{-1} and at the temperature range of 303 - 333 K. From the results obtained, it was observed that ET gums inhibited the dissolution of mild steel in the acid medium. Thermodynamic parameters obtained from the studies revealed the corrosion inhibition process to be spontaneous, exothermic and physisorptive. The adsorption of ET gums on the steel surface aligned well with the Langmuir, Freundlich and Temkin isotherm models**.** Linear polarization results revealed that ET functioned as a mixed-type inhibitor by inhibiting both the cathodic and anodic reactions on the mild steel surface.

Corresponding Author*
E-Mail: momohbat2007@gmail.com
[a] Department of Chemistry, Federal University of Agriculture, P.M.B.2373 Makurdi, Nigeria.

Introduction

Corrosion is the process through which metals/alloy deteriorates. The presence of moisture, acids, bases, salts, aggressive metal polishes and electrolytes generally would lead to the deterioration of most metals/alloys. According to Ahmad and Roberge,[1,2] the tendency of a metal/alloy to corrode to a large extent is a function of the type of metal/alloy and the aqueous medium.

Mild steel is known for its widespread industrial applications due to its structural and mechanical properties. It is, however, susceptible to corrosion when it gets in contact with electrolytes resulting in a relatively short life span.[1,2] Corrosion of steel structures and pipes result in significant losses of products in industries, environmental pollution and ecological disasters which have attracted much attention and investigations.[3,4]

A substance is said to be a corrosion inhibitor when on its addition to a corrosive environment, it either slows down or prevents corrosion. These substances can function by adsorbing both physically and chemically at the metal/solution interface thereby serving as a barrier between the metal and the corrosive species in the environment.[5-7] Peter et al. and Ramyan *et al.*,[7,8] described corrosion inhibitors as usually possess heteroatoms such as oxygen, nitrogen and sulfur that have hydrocarbon parts that are typically attached to or part of a polar group, an aromatic ring or a conjugated system.

Many inorganic and organic compounds have been used and are still being employed in mitigating corrosion of metals and alloys. However, most of these compounds are expensive coupled with the fact that they pose health and environmental challenges hence the quest for cheap and environmentally friendly inhibitors as substitutes.[5,7,8]

Plant gums have been reported as good corrosion inhibitors against the dissolution of steel in acidic environments.[9-14] Umoren has investigated the inhibitive effects of plant gum exudates from *Raphiahookeri* (RH) against the corrosion of mild steel in $H_2SO_4$and Ebenso.[9] The results obtained revealed that RH acted as a suitable corrosion inhibitor for the corrosion of mild steel in sulphuric acid medium. Abdallah[10] investigated the potential of *Guar gum* (GG) as a corrosion inhibitor for carbon steel in 1.0 MH_2SO_4 solution using weight loss and Tafel polarization techniques. The results showed that GG inhibited the corrosion of carbon steel in the acid medium and acted as a mixed type inhibitor. In other studies, other gums such as *Gum arabic* (GA), *Albizia zygia (AZ), Anogessus leiocarpus(Al) and Ficus platphylla* (FP) have also been reported to be good corrosion inhibitors.[11-14]

The results of phytochemical and pharmacological studies carried out by Prabha *et al.*, and Prashant and Shital on *Euphobia tirucalli* (ET) gum exudates showed that the gum exudates contain triterpenes, diterpene esters, steroids, alkaloids, flavonoids, tannins, phenols, anthraquinones and cardiac glycosides[15,16] which are sources of heteroatoms.

This study sets to investigate the kinetics and thermodynamics of the dissolution of mild steel in 1.0 M solution of HCl in the absence and presence of *Euphobiatirucalli* gums using weight loss and linear polarization measurements.

Experimentals

Mild steel coupons of dimension 3x2 cm^2 and percentage composition: Si-0.03 %, P-0.04 %, S-0.04 %, Mn- 0.60 % and the rest Fe, were used for this study. Analar grade reagents were used for the study.

Purification of *Euphobia tirucalli* gum.

The procedure adopted for the purification of gum has been reported elsewhere by Femi et. al., and other researchers.[17,18] The gums were oven dried at 40 °C for two hours after which they were pulverized with a blender and hydrated in chloroform water of double strength for five days with intermittent stirring such that all the gums particles dissolve completely. A 75 μm sieve was used to strain the hydrated gums to obtain a pure slurry which was allowed to sediment. Absolute ethanol was used to precipitate the gum sediment from the slurry which was later filtered and defatted using diethyl ether. The precipitate was dried again by placing it in an oven at the temperature of 40 °C for 48 hours, after which the dried flakes were pulverized using a blender. The pulverized gums were kept in a dry and air tight container. Inhibitor test solutions (0.2, 0.4, 0.6, 0.8 and 1.0 g L^{-1}concentrations)[19] were prepared by dissolving appropriate quantities (0.05 g - 0.25 g) of the gum exudates in 250 mL of 1.0 M HCl solution.

Weight loss measurement

Mild steel coupons were cleaned, weighed and immersed in 250 mL test solutions in the absence and presence of ET gum exudates (0.2, 0.4, 0.6, 0.8and 1.0g L^{-1}) as reported in previous studies.[19,20] They were removed at specified time intervals, washed in water, cleaned with ethanol, dried with acetone and reweighed. The average loss in weight was taken as the difference between the initial and final weights of the mild steel (in duplicates).

The corrosion rate of mild steel as a function of time was investigated by carrying out the experiment for 24 – 168 hours. This was done in the absence and presence of ET exudates. Temperature studies were done in a similar manner for three hours with the water bath maintained at 303- 333 K.

By carrying out the necessary substitutions in equations 1 to 3, weight loss data were used to evaluate the weight loss (g h^{-1}), corrosion rate (g h^{-1} cm^{-2}), inhibition efficiency (% *IE*) and the degree of surface coverage (θ).

$$CR(gh^{-1}cm^{-2}) = \frac{\Delta W}{At} \qquad (1)$$

$$IE(\%) = 100\left(1 - \frac{W_1}{W_2}\right) \qquad (2)$$

$$\theta = 1 - \frac{W_1}{W_2} \qquad (3)$$

where $\Delta W = W_2 - W_1$ is the weight loss of mild steel after time, *t*, W_1 and W_2 are the weight loss (g) of mild steel with and without the inhibitor, respectively, θ is the extent of surface coverage of the inhibitor, *A* is the area of the metal coupon (in cm^2) and *t* is the immersion period (in hours).[6]

Linear polarization measurements

The coupons of 3 x 2 cm^2 dimension were sealed with epoxy resin in such a way that only 1 cm^2 was left exposed. A three-electrode system consisting of mild steel as working electrode, platinum (Pt) as an auxiliary electrode and saturated calomel electrode (SCE) as a reference electrode was used. Linear polarization studies were carried out using Metrohm Autolab AUT50280 in the potential range of -1500 to 1500 mV with a scan rate of 0.012 V s^{-1} at room temperature.

The linear Tafel segments of the anodic and cathodic curves were extrapolated to corrosion potential to obtain the corrosion current densities (I_{corr}). The % *IE* was obtained from the equation below:

$$\%IE = 100\ \frac{I_{corr(\text{blnk})} - I_{\text{corr(inh)}}}{I_{\text{corr(blnk)}}} \qquad (4)$$

where $I_{\text{corr(blank)}}$ is the corrosion current density of MS in the free acid solution and$I_{\text{corr(inh)}}$ is the corrosion current density of MS in the inhibited acid solution.[7]

Optical microscopy

The morphologies of the surface of the polished mild steel coupons before immersion in the test solutions and after immersion in the test solutions were investigated using a metallurgical microscope (Tsview digital metallurgical microscope, model: Tucsen 0923502).

Results and discussion

The corrosion rate of mild steel and inhibition efficiency of ET gums

Figure 1 showed the rate of corrosion of mild steel in the free acid and inhibited 1.0 M HCl solution as a function of immersion time. It can be observed from the plot in Figure 1 that the rate of corrosion of the steel decreased with immersion time and as the concentrations of ET gums increased.

Figure 2 illustrates the trend of inhibition efficiency (% *IE*) of various concentrations of ET gums with immersion time. Inhibition efficiency of the gums increased as the concentrations of ET gums increased with % IE > 98 up to the immersion time of 96 h before decreasing.

This trend may be due to the desorption of the constituents of ET gums from the surface of the steel over a prolonged exposure resulting in the inhibition efficiency been lowered as observed in the plots.

Olasehinde *et al.*, and Momoh-Yahaya *et al.*[20,21] in previous studies reported the decrease in inhibition efficiency of *Nicotiana tabacum* extracts and adenine

molecules in acidic environments at more extended immersion periods.

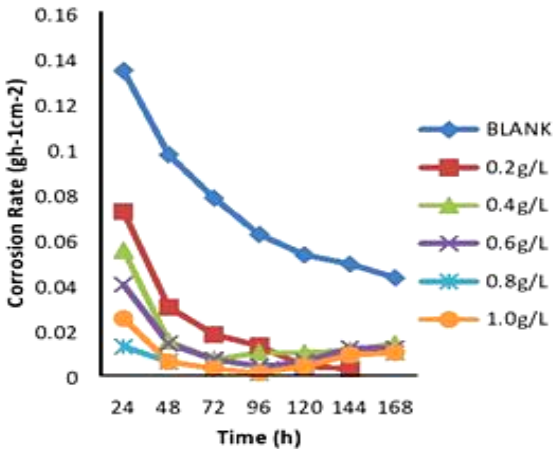

Figure 1. The corrosion rate of mild steel as a function of time in the absence and presence of ET gums

In both studies, the desorption of the constituents of *Nicotiana tabacum* extracts and adenine molecules from the surface of the mild steel was attributable to the decrease in inhibition efficiency observed.

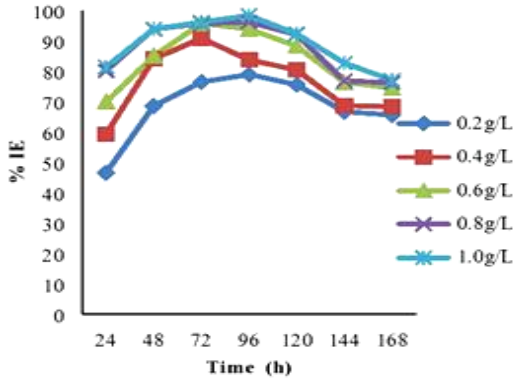

Figure 2. Inhibition efficiency of ET gums as a function of time (h).

Temperature considerations

Figure 3 showed the trend in the rate of corrosion of mild steel in uninhibited and inhibited 1.0 M solution of HCl at 303 - 333 K. The plots reveal that the rates of corrosion of mild steel increased generally at higher temperature values both in the free acid solution and in the presence of ET gums. Thermodynamically, the average kinetic energy of reacting species in a system is a function of the temperature. Reacting species become more energetic with a rise in temperature, this explains the increased rates of dissolution and corrosion rates of the mild steel in both the uninhibited and inhibited test solutions at higher temperatures. Other researchers corroborate this observation.[20-23] However, the rate of corrosion of mild steel was relatively lower in the inhibited test solutions compared with the uninhibited acid solution. This signifies the inhibitive effect of ET gums on the acid corrosion of mild steel.

The plot of the inhibition efficiency of ET gums as a function of temperature (303-333 K) is presented in Figure 4. The plot shows a decrease in inhibition efficiency of ET gums as the temperature of the system was increased. This could be attributed to the agitation of adsorbed ET gums and consequent desorption of ET gums from the mild steel surface as temperature increased.[20-22] The lowering of inhibition efficiency values with increasing temperature is associated with a physisorptive mechanism of adsorption as reported in other works.[20-24]

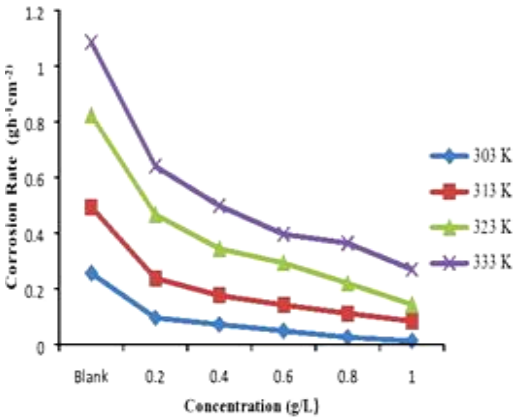

Figure 3. The corrosion rate of mild steel in 1.0 M HCl as a function of the concentration of ET gums at 303-333 K.

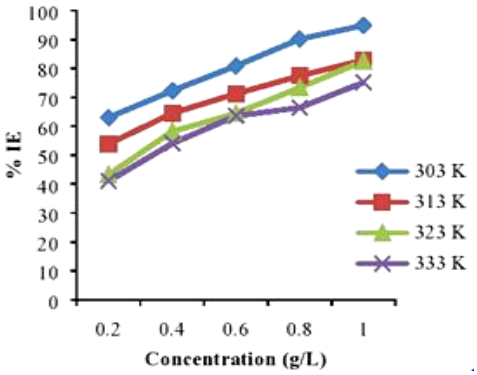

Figure 4. Inhibition efficiency of ET gums as a function of concentration at 303- 333 K.

The relationship between the corrosion rate of mild steel in the various test solutions and the temperature was evaluated using the Arrhenius equation (*equation* 5). Taking logarithm of both sides of equation 5, equation 6 is obtained.

$$CR = A\exp - E_a / RT \quad (5)$$

$$\log CR = \log A - \frac{E_a}{2.303RT} \quad (6)$$

where *CR* is the rate of corrosion of the metal, *A* is the Arrhenius or pre-exponential factor, E_a is the apparent effective activation energy, *R* is the universal gas constant and *T* is the absolute temperature of the system (K).

A plot of log *CR* versus 1/*T* represented on Figure 5 gave a straight line graph with a slope of ($-E_a/2.303RT$) and an intercept of [log *A*] from which the values of the apparent activation energy (E_a) were evaluated.[21,23,24] The values of E_a are shown in Table 1. It is evident from Table 1 that the value of E_a in the uninhibited system increased on the addition of ET gums as reflected in the values of E_a in the inhibited systems. This behavior is suggestive of a physisorptive kind of adsorption mechanism whereby an increase in temperature leads to the desorption of the adsorbed inhibitor from the steel surface thereby exposing the mild steel surface to the acid solution and leading to arise in the rate of corrosion of the steel as reported bySzauer and Brandt along with other researchers.[25,23,24]

Enthalpy ($\Delta H^{\#}$) and entropy ($\Delta S^{\#}$) of activation of the corrosion inhibition were calculated using the Eyring equation;

$$\log\frac{CR}{T} = \left[\log\left(\frac{R}{nh}\right) + \left(\frac{\Delta S^{\#}}{2.303R}\right)\right] - \frac{\Delta H^{\#}}{2.303RT} \quad (7)$$

where *CR* is the corrosion rate at temperature *T*, *R* is the molar gas constant, *n* is Avogadro's constant 6.0225×10^{23} and *h* is the Planck's constant (6.6261×10^{-34} J s). A plot of log *CR*/*T* versus 1/*T* as shown in Figure 6 is a straigh line graph with a slope of ($-\Delta H^{\#}/2.303R$) and an intercept of [$\log(R/nh) + \Delta S^{\#}/2.303R$] from which the values of $\Delta H^{\#}$ and $\Delta S^{\#}$ were calculated.[21,23,24]

The results presented in Table 1 show that the enthalpies of activation are all negative which reveals the exothermic nature of the dissolution process of the mild steel. Also, the entropies of activation were all negative for the gums.[7] Negative values of $\Delta S^{\#}$ have been reported by Refat andIshaq[25] to represent the association mechanism of the corrosion process whereby a decrease in disorder takes place ongoing from the reactants to the activated complex. Shukla and Ebenso corroborate this explanation in their findings on the adsorptive behavior and thermodynamic properties of streptomycin in the corrosion of mild steel in1.0 M HCl.[23] In their study, the values of $\Delta S^{\#}$ were not only negative but higher in the inhibited systems.

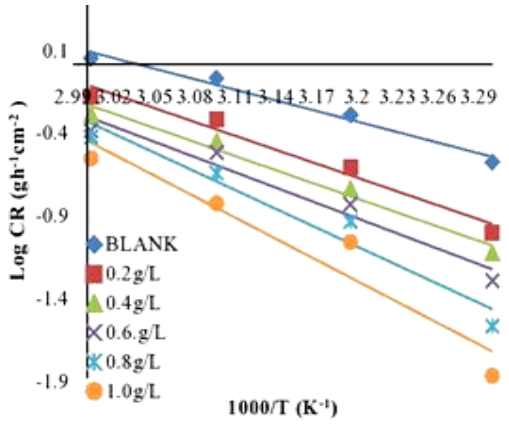

Figure 5. Arrhenius plot of the temperature -dependence of the corrosion rate of mild steel in 1.0 M HCl in the absence and presence of ET gums.

The values of $\Delta S^{\#}$ in this study (Table 1) aligns with the findings of Shukla[23] and Refat.[25] The entropy of activation, $\Delta S^{\#}$ in this present study increased in the presence of ET gums. This may be as a result of the adsorption of ET gums on the surface of the steel thereby slowing the discharge of hydrogen ions on the surface of the mild steel and the rate of corrosion of the steel.[23-25]

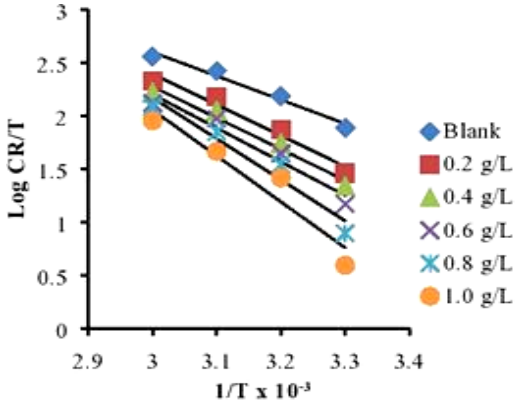

Figure 6. Eyring plot of the temperature-dependence of the corrosion rate of mild steel in 1.0 M HCl in the absence and presence of ET gums.

Table 1. Thermodynamic parameters of the corrosion of mild steel in 1.0 M HCl in the presence and absence of ET gums at 303-333 K.

Concentration, g L^{-1}	E_a, kJ mol^{-1}	$\Delta H^{\#}$, kJ mol^{-1}	$\Delta S^{\#}$, J mol^{-1} K
Blank	16.280	-4.509	-132.0
0.2	20.104	-5.569	-113.6
0.4	20.736	-5.774	-108.1
0.6	22.457	-6.220	-66.01
0.8	25.941	-7.185	-75.45
1.0	29.018	-8.037	-68.69

Adsorption isotherms

Surface coverage (Θ) values derived from weight loss measurements were adapted into various adsorption isotherms in order to know the adsorption characteristics of ET gums. The Langmuir, Freundlich and Temkin isotherms were found to give good descriptions of the adsorption characteristics of ET gums with all the plots having linear slopes and regression coefficients values $R^2 \geq 0.9$.[5,23] The functionalized and linear forms of the Langmuir, Freundlich and Temkin isotherm models[5] are the followings:

Isotherm	Functional form	Linear form
Langmuir	$k_{ads}C = \frac{\theta}{1-\theta}$	$\frac{C}{\theta} = C + \frac{1}{k_{ads}}$
Freundlich	$k_{ads}C^n = 0$ $(0 < n < 1)$	$\log\theta = \log k_{ads} - n\log C$
Temkin	$k_{ads}C = \exp(f\theta)$	$-2\alpha\theta = 2.303(\log k_{ads} - \log C)$

where C is the concentration of the inhibitor in the bulk electrolyte, K_{ads} is the adsorption equilibrium constant, Θ is the degree of surface coverage of the inhibitor and ∝is the molecular interaction parameter.[20] Table 2 presents the adsorption parameters evaluated from the plots.

The adsorption equilibrium constant, K_{ads} is related to the standard free energy of adsorption, ΔG_{ads} as showed in equations 8 and 9,

$$\log K_{ads} = -1.744 - \frac{\Delta G^0_{ads}}{2.303RT} \quad (8)$$

$$\Delta G_{ads} = -2.303RT \log(55.5K_{ads}) \quad (9)$$

where ΔG_{ads} is the standard free energy of adsorption of ET gums on the mild steel surface, R is the universal gas constant, 55.5 is the concentration of water in solution in mol L^{-1} and K_{ads} is the equilibrium constant of adsorption. The values of ΔG^0_{ads} were negative and less than -20 kJ mol^{-1} for all the three adsorption models.

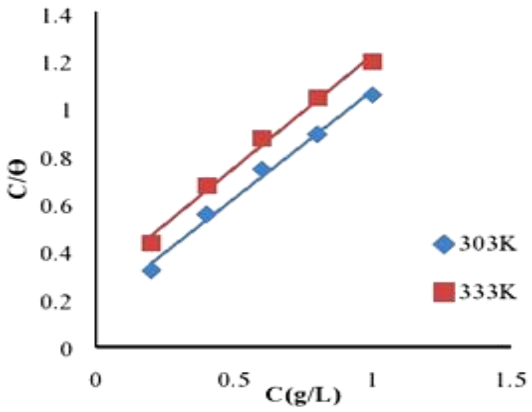

Figure 7. Langmuir isotherm for the adsorption of ET gums on mild steel surface at 303 K and 333 K respectively.

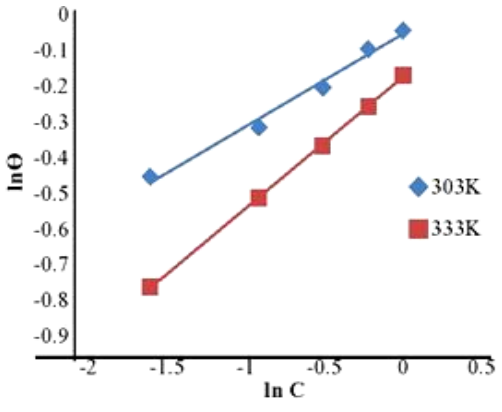

Figure 8. Freundlich isotherm for the adsorption of ET on mild steel surface at 303 K and 333 K respectively.

This implies that the adsorption of ET gums on the surface of the mild steel coupon is spontaneous and physisorptive.[7] The values of $\Delta G^0_{ads} \leq$-20 kJ $mol^{-1}$and $\Delta G_{ads} \geq -40$ kJ mol^{-1} have been reported in studies conducted by Momoh-Yahaya *et al.* and Oguzie *et al.* to signify the mechanisms of physisorption and chemisorption respectively.[21,5]

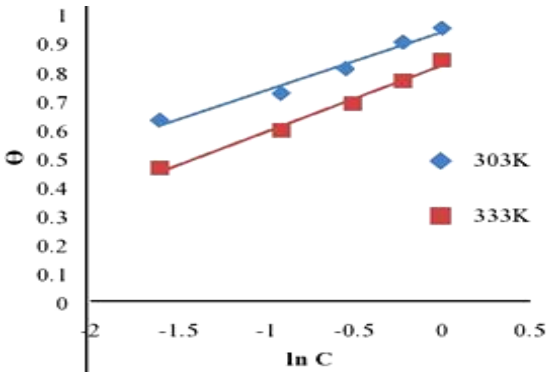

Figure 9. Temkin isotherm for the adsorption of ET on mild steel surface at 303 K and 333 K respectively.

Linear polarization

Linear polarization plots for the corrosion of mild steel in the various test solutions are shown in Figure 10 while Table 3 presents all the linear polarization parameters derived from the polarization plots and inhibition efficiency values.

The corrosion current density is a function of the reactivity of a metal in an aqueous environment. The higher the values of I_{corr}, the higher the dissolution of the metal and vice versa. Addition of ET gums is observed to reduce the anodic and cathodic current densities and the corresponding corrosion current density (I_{corr}) by shifting the corrosion potential (E_{corr}) toward more negative (cathodic) values.

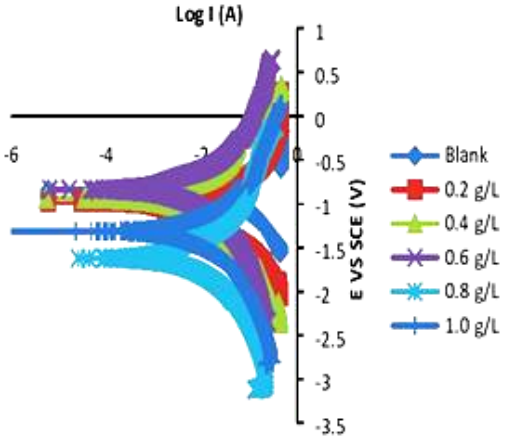

Figure 10. Linear polarisation plots of mild steel in 1.0 M HCl in the absence and presence of ET.

These shifts in the corrosion potential (E_{corr}) are more pronounced at higher ET concentrations, and the cathodic inhibiting effect becomes more significant. This implies that the gums functioned as a mixed-type inhibitor, with predominant cathodic effect.

Table 2. Adsorption parameters of ET gums on mild steel surface in 1.0 M HCl

	Temperature, K	**Slopes**	**Intercepts**	R^2	α	K_{ads}	ΔG_{ads}, **kJ mol^{-1}**
Langmuir	303	0.904	0.169	0.991	-	5.921	-14.60
	333	1.076	0.276	0.990	-	3.376	-14.49
Freundlich	303	0.625	-0.2264	0.977	-	1.684	-11.43
	333	1.050	-0.608	0.976	-	4.051	-14.10
Temkin	303	0.324	0.778	0.934	0.324	11.04	-16.17
	333	0.292	0.535	0.949	0.292	6.23	-16.18

Table 4. Linear polarisation parameters for the corrosion of mild steel in 1.0 M HCl in the absence and presence of ET.

Conc., g L^{-1}	E_{corr}, **mV**	I_{corr}, **µAcm^{-2}**	$^{\beta}$**a,V dec^{-1}**	$^{\beta}$**c, V dec^{-1}**	***CR*, mmyr^{-1}**	**%*IE***
Blank	-843.79	299.86	0.47551	0.31335	348.44	-
0.2	-513.90	135.76	0.64010	0.54541	157.75	54.73
0.4	-844.30	266.10	0.52436	0.29977	147.12	57.78
0.6	-836.65	22.93	0.35607	0.32226	26.643	92.35
0.8	-1620.4	17.81	0.25595	0.28927	20.692	94.06
1.0	-1315.2	20.31	0.26930	0.23854	23.599	93.23

The values of b_a and b_c changed as the inhibitor concentration increased, signifying the influence of ET gum exudates on both the dissolution of the mild steel in 1.0 M HCl and the kinetics of hydrogen evolution. This is revealed in similar studies by Oguzie *et al*. and others.[3-5,30]

Linear polarization

Linear polarization plots for the corrosion of mild steel in the various test solutions are shown in Figure 10 while Table 3 presents all the linear polarization parameters derived from the polarization plots and inhibition efficiency values.

The corrosion current density is a function of the reactivity of a metal in an aqueous environment. The higher the values of I_{corr}, the higher the dissolution of the metal and vice-versa. Addition of ET gums is observed to reduce the anodic and cathodic current densities and the corresponding corrosion current density (I_{corr}) by shifting the corrosion potential (E_{corr}) toward more negative (cathodic) values.

These shifts in the corrosion potential (E_{corr}) are more pronounced at higher ET concentrations, and the cathodic inhibiting effect becomes more significant. This implies that the gums functioned as a mixed-type inhibitor, with predominant cathodic effect. The values of b_a and b_c changed as the inhibitor concentration increased, signifying the influence of ET gum exudates on both the dissolution of the mild steel in 1.0 M HCl and the kinetics of hydrogen evolution. This is revealed in similar studies by Oguzie *et al.* and others.[3-5,30]

Optical microscopy

Plates I, II and III show the micrographs of the polished mild steel, the polished steel after immersion in the uninhibited acid solution and the polished steel after immersion in the inhibited acid solution respectively. Plate II shows a steel surface that is relatively damaged compared to Plates I and III. This is as a result of the rust formed on it after undergoing corrosion in 1.0 M solution of HCl in the absence of the inhibitor. The micrograph of mild steel surface in Plate III shows no pits and cracks except some polishing lines and the presence of an excellent protective film.

This further confirms the adsorption of the constituents of ET gums on the mild steel surface and the inhibitive property of ET gums against the corrosion of mild steel in 1.0 M solution of HCl.

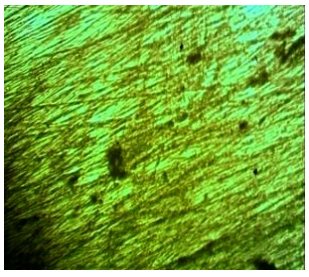

I

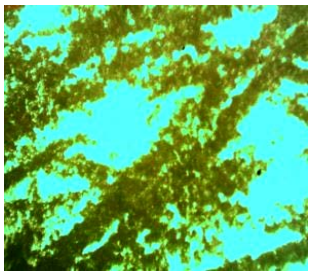

II

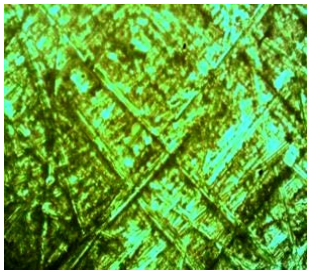

III

Plates: I -Polished mild steel; II - Polished mild steel in 1.0 M HCl; III - Polished mild steel in 1.0 M HCl with ET gums.

Conclusion

The results obtained from this study have shown that *Euphorbia tirucalli* gum exudates acted as a useful and efficient inhibitor against the dissolution of mild steel in 1.0 M HCl. Inhibition efficiency of the gums was found to be concentration dependent. However, the inhibition efficiency of the gums decreased with immersion time and rose in temperature. Values of E_a, $\Delta H^{\#}$ and ΔG_{ads} obtained showed that the adsorption of *Euphorbia tirucalli* gums exudates on the steel surface was physisorptive, exothermic and spontaneous. Linear polarization measurements showed that *Euphorbia tirucalli* gum exudates functioned as a mixed corrosion inhibitor by inhibiting and retarding the rates of both the anodic metal dissolution and cathode hydrogen ion reduction reactions. Optical micrographs confirm the adsorption of *Euphorbia tirucalli* gum exudates on the surface of the mild steel.

References

[1]Ahmad, Z., *Principles of corrosion engineering and corrosion control*.Butterworth-Heinemann: Elsevier Science and Technology Books, **2006.** https://www.elsevier.com/books/principles-ofcorrosion-engineering-and-corrosion-co...

[2]Roberge, P. R., Handbook of corrosion engineering. New York McGraw-Hill, **2000**. https://www.cntq.gob.ve/cdb/documentos/quimica/197.pdf.

[3]Okafor, P. C., Liu, X., Zheng, Y. G., Corrosion inhibition of mild steel by ethylaminoimidazoline derivative in CO2-saturated solution, *Corros. Sci*., **2009**, *51(4)*,761-768. https://doi.org/10.1016/j.corsci.2009.01.017

[4]Arora, P., Kumar, S., Sharma, M. K., Mathur, S. P., Corrosion Inhibition of Aluminium by Capparis decidua in Acidic Media, *E-J.Chem*., **2007**, *4(4)***,**450-456. downloads.hindawi.com/journals/jchem/2007/487820.pdf

[5]Oguzie, E. E., Mejeha, I. M., Nwandu, M. C., Okeoma, K. B., Nnanna, L. A., Chidiebere, M. A., Eze, F. C., Experimental and theoretical assessment of the inhibiting action of Aspilia africana extract on corrosion aluminum alloy AA3003 in hydrochloric acid, *J. Mater. Sci*., **2012**, *47(6)*, 2559-2572. https://doi.org/10.1007/s10853-011-6079-2

[6]Ameh, P. O., Eddy, N. O., Gimba, C. E., *Physiochemical and rheological studies on some natural polymers and their potentials as corrosion inhibitors*. UK: Lambert academic publishing; **2012.**

[7]Peter, A., Obot, I. B., Sharma, S. K. Use of natural gums as green corrosion inhibitors: an overview, *Int. J. Ind. Chem*., **2015**, *6(3)*,153‑164. https://link.springer.com/article/10.1007/s40090-015-0040-1

[8]Ramya, K., Mohan, R., Anupama, K. K., Joseph, A., Electrochemical and theoretical studies on the synergistic interaction and corrosion inhibition of alkyl benzimidazoles and thiosemicarbazide pair on mild steel in hydrochloric acid, *Mater. Chem. Phys*., **2015**, *149–150*, 632-647. https://doi.org/10.1016/j.matchemphys.2014.11.020

[9]Umoren. S. A., Ebenso, E. E., Studies of the anti‑corrosive effect of Raphia hookeri exudate gum‑halide mixtures for aluminum corrosion in acidic medium, *Pigment Resin Technol*., **2008**, *37(3)*, 173-182. https://www.emeraldinsight.com/doi/abs/10.1108/03699420810871020

[10]Abdallah, M., Guar Gum as Corrosion Inhibitor for Carbon Steelin Sulfuric Acid Solutions, *Portugaliae Electrochim. Acta*., **2004**, *22(2)***,**161-175. http://www.peacta.org/articles_upload/PEA2222004161.pdf

[11]Umoren, S. A., Obot, I. B., Ebenso, E. E., Okafor, P. C., Ogbobe, O., Oguzie, E. E., Gum arabic as a potential corrosion inhibitor for aluminum in alkaline medium and its adsorption characteristics, *Anti-corros. Methods. Mater*., **2006**, *5(5)*,277-82. https://www.emeraldinsight.com/doi/abs/10.1108/00035590610692554

[12]Ameh, P.O., Inhibitory action of Albizia zygia gum on mild steel corrosion in acid medium, *Afr. J. Pure Appl. Chem*.,**2014**, *8(2)*,37‑46.https://doi.org/10.5897/AJPAC2014.0549

[13]Ameh, P. O., Odiongenyi, A. O., Eddy, N. O., Joint Effect of Anogessius Leocarpus Gum (AL Gum) Exudate and Halide Ions on the Corrosion of Mild Steel in 0.1 M HCl, *Portugaliae Electrochim. Acta*., **2012**, *30(4)*,235-245.http://www.scielo.mec.pt/scielo.php?pid=S0872-19042012000400001&script=sci_arttext&tlng=en

[14]Eddy, N. O., Ameh P. O. Ebenso, E. E., Chemical Information from GCMS of Ficus Platyphylla Gum and its Corrosion Inhibition Potential for Mild Steel in 0.1 M HCl, *Int. J.Electrochem. Sci*., **2012,** 7, 5677‑5691. http://www.electrochemsci.org/papers/vol7/7065677.pdf

[15]Prabha, M. N., Ramesh, C. K., Kuppast, I. J., Mankani, I. J., Studies on anti-inflammatory and analgesic activities of Euphorbia tirucalli L. Latex, *Int. J. Chem. Sci*., **2008**, *6(4)*,1781-1787.https://www.tsijournals.com/articles/studieson-antiinflammatory-and-analgesic-activitiesof-euphorbia-tirucalli-l-latex.pdf

[16]Prashant, Y. M., Shital, S. P., Euphorbia tirucalli L.: Review on morphology, medicinal uses, phytochemistry and pharmacological activities, *Asian-Pacific J. Tropical Biomed*., **2017**, 7(7), 603-613. https://doi.org/10.1016/j.apjtb.2017.06.002

[17]Femi-Oyewole, M., Musiliu, O., Taiwo, O., Evaluation of the suspending properties of Albiziazygia gum on sulphadimidine suspension, *Trop. J. Pharm. Res*., **2004**, *3(1)*,279-284.http://www.bioline.org.br/pdf?pr04003

[18]Jao, A. M., *Physicochemical and rheological characterization of some plant gum exudates and their inhibition of the corrosion of aluminum in acidic medium. M.Sc Thesis*Ahmadu Bello University Zaria, Nigeria, **2014**.http://kubanni.abu.edu.ng/jspui/bitstream/123456789/6736/1/ALIYU%20MOHAMMED%20JA%27O.pdf

[19]Chahul, H. F., Ndukwe, G. I., Abawua, S. T., Corrosion inhibition studies of mild steel with stem bark extract of maranthes polyandra (Benth.) prance, *J. Chem.Soc. Nig*., **2017,** *42(1)*,55-61.

[20]Olasehinde, E. F., Olusegun, S. J., Adesina, A. S., Omogbehin, S. A., Momoh-Yahaya, H. Inhibitory Action of Nicotiana tabacum Extracts on the Corrosion of Mild Steel in HCl: Adsorption and Thermodynamics Study, *Nature and Science*, **2012**, *10(12)*,21-34. http://www.sciencepub.net/nature/ns1101/013_13992ns1101_83_90.pdf

[21]Momoh-Yahaya, H., Eddy, N. O., Iyun, J. F., Gimba, C. E., Oguzie, E. E., Experimental Investigation of the Inhibiting Action of Adenine on the Corrosion of Mild Steel in Acidic Environments, *J. Mater. Sci. Res.*, **2013,** *2(1)*, 59-74.http://www.ccsenet.org/journal/index.php/jmsr/article/view/21307

[22]Singh, A. K., Quraishi, M. A., Piroxicam; A novel corrosion inhibitor for mild steel corrosion in HCl acid solution, *J. Mater. Environ. Sci*.,**2010,** *1(2)*,101-110.https://www.jmaterenvironsci.com/Document/vol1/13-JMES-12-2010-quraishi.pdf

[23]Shukla, S, S., Eno, E. E., Corrosion Inhibition, Adsorption Behavior and Thermodynamic Properties of Streptomycin on Mild Steel in Hydrochloric Acid Medium, *Int. J. Electrochem. Sci.*, **2011**, *6***,** 3277‑3291. http://www.electrochemsci.org/papers/vol6/6083277.pdf

[24]Szauer, T., Brandt, A., On the role of fatty acid in adsorption and corrosion inhibition of iron by amine—fatty acid salts in acidic solution, *Electrochimica Acta*, **1981**,*26(9),*1257-1260.

[25]Hassan, R. M., Zaafarany, I. A., Kinetics of Corrosion Inhibition of Aluminum in Acidic Media by Water-Soluble Natural Polymeric Pectates as Anionic Polyelectrolyte Inhibitors, *Materials*, **2013,** *6(6),*2436-2451. http://citeseerx.ist.psu.edu/viewdoc/download;jsessionid=36A5C699B41AB5618365B524408894D8?doi=10.1.1.361.4477&rep=rep1&type=pdf

Received: 18.01.2019.
Accepted: 27.02.2019.

NICKEL ACETYLACETONATE CATALYZED KNOEVENAGEL CONDENSATIONS AT ROOM TEMPERATURE

Manojkumar U. Chopade,[a]* Anil U. Chopade[b] and Santosh V. Padghan[a]

Keywords: Knoevenagel condensation, Ni(acetylacetonate)₂; benzaldehydes; ethyl cyanoacetate.

Nickel acetylacetonate (Ni(acac)₂) as a catalyst was tested in Knoevenagel condensation of benzaldehyde with ethyl cyanoacetate in DMSO to provide α-cyano ethyl cinnamate. The substituted benzaldehydes and 3-methylbutyraldehyde gave similar reaction and the corresponding products were obtained in good yields (78-92%) under clean and straightforward condition.

* Corresponding Authors
Fax: +91-2438-234395
E-Mail: chopademanojkumar@gmail.com
[a] Sant Dnyaneshwar Mahavidyalaya, Department of Chemistry, Soegaon, Dist: Aurangabad 431120 India
[b] Dahiwadi College, Dahiwadi, Rayat Shikshan Sansthan, Satara, Shivaji University Kolhapur 415508 India

Introduction

The Knoevenagel condensation is one of the most important C-C bond forming reaction, and the cyanoalkene reaction products have proved to be versatile intermediates in the organic synthesis.[1] These compounds are powerful electrophiles readily undergo Michael addition reactions and result in the synthesis of heterocyclic compounds.[2] They represent a significant functionality in organic transformations due to their easy conversion into elaborated functionalities of amines, amides, esters, lactams and lactones.[3] Moreover, conjugated cyano alkenes are important compounds due to their biological properties.[4]

There are numerous known methods to access C=C bond formation, but these reactions are mainly catalyzed by amine-quaternary ammonium salt double activation catalysts[5] and require harsh reaction conditions. The yields generally are limited. These methods particularly are unsuitable for atom economic synthesis.[6] Development of new synthetic methodologies using transition metal Lewis acid catalyst has increased importance[7] due to the numerous advantages like low cost, neutral condition, ambient temperature, high selectivity, and avoid of salt-type by-product formation. Transition metal catalysts mostly promote the activation of C-H functionalities due to their high ability to generate carbanion equivalent species.[8]

EXPERIMENTAL SECTION

Materials and methods

All reactions were carried out in dry solvents unless otherwise stated. Reactions were monitored by thin layer chromatography (TLC) on silica gel plates (Kieselgel 60 F_{254}, Merck). Visualization of the spots on TLC plates was achieved either by UV light or by staining the plates in 2,4-dinitrophenylhydrazine/anisaldehyde and charring on a hot plate. All products were characterized by ^{1}H NMR, ^{13}C NMR, IR, and mass spectrometry. ^{1}H NMR and ^{13}C NMR spectra were recorded on Varian Mercury 300 MHz spectrometer. IR spectra were obtained on a Shimadzu FTIR-8400 with samples loaded as thin films on KBr plate, neat or with CH_2Cl_2 as indicated. Mass spectra were recorded at an ionization potential of 70 eV; Melting points recorded are uncorrected. Column chromatography on silica gel (100-200 mesh) was performed with reagent grade ethyl acetate and hexane as an eluent.

Synthesis of 2-cyano-3-phenylacrylic acid ethyl ester (3a)

A mixture of ethyl cyanoacetate (531 mg, 4.7 mmol) Ni(acac)₂ (10 mg, 0.9 mol %) in DMSO (2 mL) were stirred at room temperature, aldehyde(benzaldehyde) (498 mg, 4.7 mmol), was added, the reaction mixture was further stirred for 1.0 h. The progress of the reaction was monitored by taking TLC. After completion of the reaction, the mixture was diluted with water. The reaction mixture was extracted with EtOAc (2 x 20 mL) and the organic layer was washed with brine and dried with Na_2SO_4. Evaporation of solvent furnished the crude product that was purified by column chromatography over silica gel using EtOAc in petroleum ether to give a pure solid product. Yield: 85 %, M.p.: 68 ^{0}C, IR: ν=1726 (C=O, ester) and 2225 (CN) cm^{-1}; ^{1}H NMR($CDCl_3$,TMS): δ 1.43 (t, 3H, *J*= 7.2 Hz), 4.38 (q, 2H, *J*= 7.2 Hz) , 7.53 (d, 2H, *J*= 7.8 Hz), 8.13 (d, 3H, *J*= 7.8 Hz), 8.26 (s, 1H)

The other compounds have been synthesized in an analogous way with using the solvent and reaction time given in Table 1.

Result and Discussion

The nickel acetylacetonate (Ni(acac)₂) is a crucial Lewis acid catalyst proved to be highly effective in a various organic reaction like Michael addition,[9] Grignard reactions,[10] alkylations, alkenylations,[11] aryl C-H activation coupling reactions,[12] N-arylations and C-N bond cleavage,[13] cyanoesterification[14] and homocoupling reactions.[15]

As part of our ongoing program, we inspired and encourage developing new methodologies for Knoevenagel condensation of ethyl cyanoacetate with aldehydes and

cyclic ketones. We are demonstrating first time using Ni(acac)$_2$ as a catalyst in Knoevenagel condensation reaction. The Knoevenagel condensation of benzaldehyde (**1a)** with ethyl cyanoacetate (**2)** furnished the **3a** in EtOH with good yield at ambient reaction condition in 1 h. For optimization of reaction condition, we screened the role of solvents and temperature. In EtOH at 25 ^{0}C, the **3a** was formed in 80 % yield in 8 h then reaction condition changed heating to reflux for 1 h resulted in 85% yield of **3a** on reflux condition. When the reaction was carried out in polar protic solvents like MeOH, the yield was decreased, i.e., 80 % while other polar solvents such as acetonitrile and acetone gave **3a** with good yield under the same conditions. Aprotic polar solvents like DMF gives 83 % and DMSO 85% were proved to be the best choice for these syntheses during short reaction time at room temperature.

The products were obtained in high yield with increasing temperature because of the endotherm character of the reaction. Due to enolization in DMSO as solvent[16] polar aprotic solvents (DMF and DMSO) was selected and as a result of detailed studies, DMSO was found to be the most effective solvent for promoting favorable reaction conditions. in DMSO **3a** was formed with good yield in 1 h even at room temperature.

This result demonstrated that Ni(acac)$_2$ is an effective catalyst for Knoevenagel condensation reaction, therefore we have tested its activity in the reaction of benzaldehyde with other active methylene group-containing compounds. The analogous reaction with malononitrile proceeded very fast and gave a corresponding product with excellent yield (90 %), while with ethyl acetoacetate the corresponding product was formed in moderate yields (75 %). Diethyl malonate gave very low yield 20 % even under long reaction time (12 h). It is noted that according to previous reports the presence of cyano moiety is a critical condition to generate carbon nucleophile and promote insertion of the metal into the C-H bond and hydrogen shift by metals to oxo species.[17,18]

After finding optimized solvent and reaction condition as shown in Scheme 1, we have studied the influence of the amount of catalyst in DMSO on the yield of **3a**.

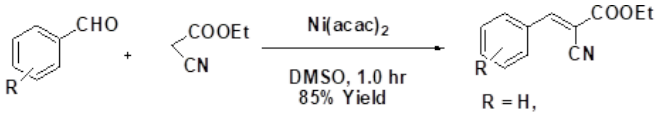

It has been observed that the model reaction did not initiate at all without the catalyst for 12 h in DMSO. The amount of catalyst used for the reaction was varied between 0.5 and 10 mol %. Decreasing the amount of catalyst loading from 10 mol % to 1 mol %, the yield of **3a** is hardly changed. The reaction rate, however, decreased and with 0.5 mol % of catalyst was found the less yield (70 %). It shows that the minimum amount of catalyst to give good results is 0.9 mol %.

The usability of Ni(acac)$_2$ catalyst was examined in the reaction of variously substituted benzaldehydes, 3-methylbutyraldehyde and cyclic ketones (cyclohexanone or cyclopentanone) with ethyl cyanoacetate. All reactions were performed in the presence of 0.9 mol% Ni(acac)$_2$ catalyst in DMSO as a solvent. The results are summarized in Table 1. There was no particular influence of the electron donating and withdrawing substituents on the yield of desirable products comparing with unsubstituted benzaldehyde.

Table 1. Synthesis of Knoevenagel condensation products in the presence of 0.9 mol % Ni(acac)$_2$ from oxo-compounds and ethyl cyanoacetate in DMSO at room temperature

Starting oxo compound	Reaction time, h	Yield, %
Benzaldehyde	1.0	85
2.5 Dimethylbenzaldehyde[a]	1.0	90
4-Methoxybenzaldehyde	1.0	87
3-Methoxybenzaldehyde	1.5	86
4-Chlorobenzaldehyde	1.3	92
4-Nitrobenzaldehyde	0.3	85
4-Bromobenzaldehyde	1.4	78
2-Nitrobenzaldehyde	0.3	80
2-Benzoloxybenzaldehyde[a]	1.3	81
3-Methylbutyraldehyde	1.0	78
Cyclopentanone	1.0	78
Cyclohexanone	1.0	78

[a]new product

Neither the acid sensitive alkoxy nor the halide substituent has any coupling or other by-reaction, but salicylaldehyde resulted in coumarin in 83 % yield under 3 h. Salicylaldehyde hydroxyl group was protected with benzyl group when the condensation reaction s proceeded under the same conditions gave above giving 81 % yield. The aliphatic aldehyde, 4-methylbutyraldehyde gave the desired product with 78 % yield in 1 h, and cyclic ketones (cyclopentanone and cyclohexanone) provided 78% and 78% yields, under 1.0 h, respectively.

Conclusion

We could demonstrate that the formation of C=C bond can be catalyzed with Ni(acac)$_2$ in a reaction of CN-group containing active methylene reactants and aldehydes or ketones under neutral condition without formation of salt-like byproducts. The present methodology can be applied in the synthesis of β-lactam type drugs.

Acknowledgment

Manojkumar Chopade is thankful to Department of Chemistry in Science and Technology, Savitribai Phule University Pune and Ajintha Education Society's for the infrastructural facility and also to CSIR, New Delhi for fellowship.

References

[1]Lehnert, W., Verbesserte variante der knoevenagel-kondensation mit TiCl$_4$/THF/pyridin(I). Alkyliden- und Arylidenmalonester bei 0–25 °C, *Tetrahedron Lett.*, **1970**, *11*(54), 4723-4724. https://doi.org/10.1016/S0040-4039(00)89377-6

[2]Volla, C. M. R., Atodiresei, I. and Rueping, M., Catalytic C–C Bond-Forming Multi-Component Cascade or Domino Reactions: Pushing the Boundaries of Complexity in Asymmetric Organocatalysis, *Chem. Rev*., **2014**, *114(4*), 2390-2431. DOI: 10.1021/cr400215u

[3]Sieber S. A., Bottcher T., β-Lactones as antibacterial agents, US8669283B2, **2008**.

[4]Approved β-lactam antibiotics are listed in FDA's Approved Drug Products with Therapeutic Equivalence Evaluations, generally known as the Orange Book http://www.accessdata.fda.gov/scripts/cder/ob/default.cfm. Current through January **2019**.

[5]Taha, N., Sasson, Y., Chidambaram, M., Phase transfer methodology for the synthesis of substituted stilbenes under Knoevenagel condensation condition, *Appl. Catal. A: Gen.*, **2008**, *350*, 217–224. https://doi.org/10.1016/j.apcata.2008.08.011

[6]Sheibani, H., Seifi, M., Bazgir, A., Three-Component Synthesis of Pyrimidine and Pyrimidinone Derivatives in the Presence of High-Surface-Area MgO, a Highly Effective Heterogeneous Base Catalyst *Synth. Commun*., **2009**, *39*, 1055–1064. DOI: 10.1080/00397910802474982

[7]Narsaiah, V., Nagaiah, K., An Efficient Knoevenagel Condensation Catalyzed by LaCl3.7H2O in Heterogeneous Medium, *Synth. Commun*., **2003**, *33*(21), 3825–3832. https://doi.org/10.1081/SCC-120025194

[8]Wan, J. P., Gan, L., Yunyun, L., Transition metal-catalyzed C–H bond functionalization in multicomponent reactions: a tool toward molecular diversity, *Org. Biomol. Chem.*, **2017**, 15, 9031-9043. DOI: 10.1039/C7OB02011B

[9]Chopade M. U., Chopade A. U., $NiCl_2$:Sparteine Catalysed Enantioselective Michael Addition of Diethyl Malonate on β-Nitrostyrene: Concise Synthesis of (R)-Rolipram, *J. Chem. Chem. Sci.* **2015**, *5*, 585-590.

[10]Terao, J., Watanabe, H., Ikumi, A., Kuniyasu, H, Kambe, N., Nickel-Catalyzed Cross-Coupling Reaction of Grignard Reagents with Alkyl Halides and Tosylates: Remarkable Effect of 1,3-Butadienes, *J. Am. Chem. Soc.* **2002**, *124*(16), 4222–4223. DOI: 10.1021/ja025828v

[11]Quan, M., Wang, X., Wu, L., Ilya, D. G., Yang, G, Zhang, W., Ni(II)-catalyzed asymmetric alkenylations of ketimines, *Nature Commun*., **2018**, 9, 2258. https://doi.org/10.1038/s41467-018-04645-3

[12]Cai, X. H., Bing, X., Recent advances in nickel-catalyzed C–H bond functionalized reactions, *ARKIVOC* **2015** (i), 184-211. DOI: http://dx.doi.org/10.3998/ark.5550190.p008.915

[13]Ilies, L., Matsubara, T., Eiichi, N. E., Nickel-Catalyzed Synthesis of Diarylamines via Oxidatively Induced C–N Bond Formation at Room Temperature, *Org. Lett.*, **2012**,*14*(21), 5570–5573. DOI: 10.1021/ol302688u

[14]Hirata, Y., Yada, A., Morita, E., Nakao, Y., Hiyama, T., Ohashi, M., Ogoshi, S., Nickel/Lewis Acid-Catalyzed Cyanoesterification and Cyanocarbamoylation of Alkynes, *J. Am. Chem. Soc*., **2010**, *132*(29),10070–10077. DOI: 10.1021/ja102346v

[15]Nakamura, K., Tobisu, M., Chatani, N., Nickel-Catalyzed Formal Homocoupling of Methoxyarenes for the Synthesis of Symmetrical Biaryls via C–O Bond Cleavage, *Org. Lett.* **2015**, *1*(24), 6142–6145. DOI: 10.1021/acs.orglett.5b03151

[16]Chopade, M. U., Magar R. R., Choudhare S. S., Padghan S. V., Development of Drug Intermediates *via* Alkylation Using Fe(acac)3 as Transition Metal Catalyst. , *J. Chem. Chem. Sci.* **2015**, *5(12)*, 682-687.

[17]Takaya, H., Yoshida, K., Isozaki, K., Terai,H., Shun-Ichi Murahashi, S. I. Transition-Metal-Based Lewis Acid and Base Ambiphilic Catalysts of Iridium Hydride Complexes: Multicomponent Synthesis of Glutarimides, *Angew. Chem. Int. Ed.* 2003, 42, 3302 –3304. DOI: 10.1002/anie.200351689

[18]Schneider, E. M., Zeltner M, N. Kranzlin, Grassa, R. N., Stark, W. J. Base-free Knoevenagel condensation catalyzed by copper metal surfaces, *Chem. Commun*., 2015, 51, 10695. DOI: 10.1039/c5cc02541a.

Received: 20.02.2019.
Accepted: 04.03.2019.

CHANGES IN MICROBIOTA, MORPHOHISTOCHEMICAL, BIOCHEMICAL SHIFTS IN MICE ON THE SODIUM DEXTRAN SULPHATE – INDUCED NONSPECIFIC ULCERATIVE COLITIS AND THE EFFECTS OF FREE PROBIOTICS AND IMMOBILIZED FORMS WITH ZEOLITE

A. A. Agababova[a], N. Kh. Alchujyan[a], A. M. Hakobyan[a]*, A. G. Gevorkyan[b] and V. H. Barsegyan[a]

Keywords: Nonspecific ulcerative colitis, sodium dextran sulphate, gastrointestinal tract, probiotic, zeolite, lipid peroxidation, microbiota, intestinal –cerebral axis, inflammation.

Acute, inflammatory processes contribute to the fact that conventionally pathogenic and pathogenic microorganisms colonize the mucous membranes of the small intestine and form biofilms, can become a source of bacterial toxin, which, when the epithelial layer breaks, penetrates to the lymphatic and blood systems, contributing to the formation of sepsis. The barrier function of the epithelium is critical in the development of inflammatory bowel diseases, while normal functioning requires a constant balance between reactivity and tolerance to microorganisms of the intestinal lumen. Increased permeability of the intestinal mucosa is the main risk factor for the spread of bacteria. Epithelium, being an essential element of tissue barriers, provides selective transport for the movement of ions and macromolecules, and also creates an obstacle for their penetration into the underlying tissues. Control of the permeability of the epithelial layer is carried out by the apical intercellular complex - tight contacts, which comprise proteins of the claudine family. Intestinal flora affects the sensory, motor and immune functions of the intestine, and also interacts with higher nervous centers. Immunosuppressive processes are one of the main causes of destabilization of the barrier function, intestine, and brain.

*Corresponding Authors
Fax:
E-mail: agnessa.agababova@bk.ru
[a] H. Buniatian Institute of Biochemistry NAS RA, 5/1 P. Sevak St., 0014, Yerevan, Republic of Armenia.
[b] M. Herazi Yerevan State University, Republic of Armenia.

INTRODUCTION

The intestinal - cerebral axis (ICA) is a bi-directional communicative system through which the brain models the functions of the gastrointestinal tract (GIT) and vice versa. ICA is based on neuronal, endocrine and immunological mechanisms connected with each other at the organism, organ, cellular and molecular level.[1] The relationship between cerebral microbiota of the intestine is one of the examples of the cooperation of the endocrine, nervous systems and nonspecific natural immunity, the importance of which for the organism in norm and in pathology is difficult to overestimate.

The gastrointestinal tract is closely related to the hypothalamic-pituitary tract through the release of peptides that control the brain's response, and also through neuroendocrine and sensory signals from the intestine. The microbiota affects the development of cognitive functions and the hypothalamic-pituitary response to the stress. Intestinal bacteria in the process of metabolism form serotonin, melatonin, amino acids, catecholamine, histamine, acetylcholine, partially being the most important neurotransmitters .[1,2,3]

The intestinal-cerebral axis is also traced in infections and inflammations that lead to mood changes and cognitive dysfunction. In particular, the brain is able to identify the introduction of pathogenic microbes in the digestive tract and respond with a sense of anxiety and restlessness. The only mechanism capable signalize the brain of danger is hematological. The sensory neurons of the vagus nerve are contacted by submucosal immune cells and project the nerve endings into the mucous membrane of the gastrointestinal tract, the site of direct interaction between the organism and the pathogen.

The detection of Fos protein, synthesized by neurons including and markers of functional activity, in the sensory neurons of the nerve after inoculation of bacteria, testified that this connection is also accomplished by the vagus nerve.[4,5] The death of intestinal neurons and glia damage with alteration of the expression of the acidic fibrillar protein and increased expression of the molecules of the main histocompatibility complex of the second class were noted in Crowns' disease, ulcerative colitis, necrotizing enterocolitis and diabetes.[6]

The purpose of this work was to study the effect of the complex positions of dextran sodium sulfate on the intestinal microbiota of mice, to obtain a model of nonspecific ulcerative colitis (NUC), to interrelate the axis of the intestine-blood-brain, the ways of affecting some zeolites of this domestic production, the immune active and anti-inflammatory properties of zeolites, found in the regions of Armenia in the experimental models of the NUC.

EXPERIMENTAL

Chemicals and reagents: Dextran sulphate 40 sodium salt (DSS), Mr 40 000, and bovine serum albumin were from Carl Roth, dextran (Mr 70 000) (Serva, Heidelberg

Germany). Sodium citrate anticoagulant, thiobarbituricacid, HEPES, 1.4-dithiothreitol, hematoxylin and eosin were purchased from Sigma-Aldrich Chemical Co.

Animals and treatmants: All procedures involved animals were in accordance with the International Laboratory Animal Care and the European Communities Council Directive (86/809/EEC) and approved by the respective local committee on biomedical ethics (H. Buniatian Institute of Biochemistry, Yerevan, NAS RA). The 2-to 3-month-old male mice from our breeding colony were used. All animals were maintained on a 12 h light/dark cycle at normal room temperature and housed in groups of 6/cage with free access to food and tap water.

Experimental design: To induct nonspecific ulcerative colitis induction, the animals were randomly divided into groups (n=12). Group I was contol group of native mice. Other groups were experimental groups with DSS-induced nonspecific ulcerative colitis.

Group II - mice received ad libitum 2.5% DSS dissolved in regular tap water for 7 days and examined immediately at the end of sodium dextran sulphate treatment.

GroupIII - a group of sodium dextran sulphate-induced nonspecific ulcerative colitis mice left untreated for the duration of 2 weeks in parallel to treated ones and referred as self-recovery to assess self-healing mechanism

Group IV-VI were of mice that were fed with 2.5 % DSS dissolved in regular tap water for 7 days and then given daily per os (through a flexible polypropylene gavage) separately probiotics, and/or probiotics immobilized with zeolites (PBZ). Control mice were given water only. On day 8, mice were sacrificed and monitored for colitis.

Probiotic strains and growth conditions: A commercially available probiotic, a concentrated source of naturally occurring microorganisms were used. *L. rhamnosus* strain B-6778 and *Bifidobacterium bifidum* strain AC-1666 (RF), as well as *L. plantarum* strain B-2353 (RF), *L. acidophilus* Er317/402 "Narine" (RA), *L. salivarius* B-7701 possessing fungicidal activity and *E. coli* Nissle1917 strain were rehydrated in sterile 0.85% NaCl and routinely propagated at 37° C in MRS medium (Hi Media, India) pH of 6.5 ± 0.2. Limiting dilution assay (based on the method of McCrady) was used for the separation, characterization, and quantification of bacteria.[7] Viability was confirmed by culturing 1 mL of the hydrated mixture on plates supplemented with MRS + agar at 37°C for 24 h. For immobilization of probiotics the culture medium was enriched with 5% of the chemically modified micronized natural mineral composition (vide infra). The probiotic mixture contained equal quantities the mentioned microorganisms (6 x 109 CFU/mL in total).

Natural mineral composition. Natural minerals mined in Armenia were used viz., zeolites from Noyemberyan, bentonite from Ijevan and diatomite from Jadzor. Their multi-elemental composition at the trace and ultra trace levels have been determined and previously modified chemical composition (zeolite (80%), diatomite (10%), and bentonite (10%)) used as efficient stimulators and carriers of the probiotics.[8] High pressure micro powder mill was used to produce about 50 μm powder from the mentioned minerals.

Evaluation of experimental colitis. The animals were weighed and monitored for the appearance of diarrhea and blood in the stool throughout the experimental period. The overall disease severity was assessed by a clinical scoring system and the disease activity index score was calculated for each animal.[9] Assessment includes 3 parameters, difference in weight before and after receiving DSS (0 = weight gain ≥ 1g: 1 = weight gain <1g; 2 = weight loss <1g; 3 = weight loss ≥ 1g); stool consistency (0 = normal stool; 1 =soft but formed stool, 2 = liquid stool); the presence of blood in the perianal region (0 = no sign of blood; 1 = signs of blood in perianal region; 2 = presence of blood in perianal region). The minimum score is 0, maximum is 7. After decapitation colon is excised opened longitudinally, rinsed with saline, and the length was measured and considered as an additional index for colitis, as well as macroscopic damage of the colonic mucosa scored based on the degree of inflammation and the presence of edema and/or ulcerations (0 = normal; 1 = slight inflammation; 2 = moderate inflammation and/or edema and 3 = heavy inflammation and/or ulcerations).[10] Toward the end of the treatment, before decapitation, all of the animals underwent a behavioral testing in open field (OP) and elevated plus-maze (EPM).

Behavioral examination: For open field test the mice were placed singly into an open field (diameter 1 m, divided by 2 concentric circles into 16 equal sections on the floor of the arena) and observed in 3 min to measure locomotor activity (the number of sectors crossed with all paws (crossing), the number of rears (posture sustained with hind-paws on the floor), grooming (including washing or mouthing of forelimbs, hind-paws, body and genitals) (exploratory behavior) and boluses (anxiety) counted manually/visually.[11]

For elevated plus-maze test, immediately after the open field test the mice were placed singly into a common central platform (10 cm × 10 cm) of elevated plus-maze comprised two open and two closed arms (45 cm x 10 cm x 10cm) and elevated to a height of 80 cm above the floor During a 3-min observation period, the following parameters were measured: number of open arms entries and number of closed arm entries. Exploration (grooming and rearing) and risk assessment (number of hanging over the open arms) were also examined. At the end of each trial, the open field and elevated plus maze were wiped clean with ethanol.

Microbiological method: Our research was carried out in accordance with the methodological decree on microbial diagnosis of diseases cause by enterobacteriaceae. Methodological decree is composed of the RF Center for Health doctors training, RF Center for Health epidemiology research institute, RF Central for Health vaccine and serum research institute after E. E. Mechnikov. Each animal was opened aseptically; samples of feces from the lower part of the colon, and brain washout were immediately placed into a clean test tube for bacteriological analysis. After decapitation trunk blood was collected and analyzed. For identification light microscopy and/or the culturing method were used for all samples. Cultures were incubated in sucrose broth at 37 °C for 24 h (blood was diluted by 1:5 v/v), then examined by microscopy, inoculated to the solid

culture media, agar plates (Endo, sucrose, and blood agar), and incubated for 24 h; blood samples incubated for 7 days, monitored daily, to facilitate a growth of microbes.[12] The following nutritional environments are used: sugar bouillon, blood agar, yolk-salt agar, Endo, Ploskirev and Saburo agars.

The identification of separated bacteria is carried out with morphological, biochemical properties, by the method of spotted series of Hiss. After the discovery of the biochemical character of microbes, which determines the family of culture and its type, is made of serological identification of microorganisms with serums until serotypes.

Histological examination: Samples for histology were excised from the brain and distal 6–8 cm of the colon, fixed in 10 % buffered formalin, and embedded in paraffin blocks. Slices with 6 μm sections were stained with hematoxylin and eosin (H&E), and scored for histological damage.[13] Pathological diagnosis of each specimen was assessed and analyzed by specialized histopathologist in a blinded manner.

Indices of oxidative stress referring to lipid peroxidation processes were established by measuring malondialdehyde (MDA) using thiobarbituric acid.[14] Samples were deproteinized with 10 % TCA, centrifuged at 15000 rpm for 3 min, and supernatants were mixed with 0.6 N HCl and 0.72 % TBA, heated for 15 min in boiling water bath with the resultant formation of pink-colored secondary product of MDA which absorbance was measured at 535 nm wavelength against reagent blank containing all the reagents minus the sample. Protein was determined using crystalline bovine serum albumin as standard.[15]

Statistical analysis: All data were analyzed using a one-way analysis of variance (ANOVA) followed by post hoc Holm-Sidak test (SigmaStat3.5 for Windows). Data are expressed as the mean±S.E.M. Statistical significance is accepted at the level $p< 0.05$.

Results and Discussion

Effect of sodium dextran sulphate in mice, histopathological shifts

In the control group of mice, there were no abnormalities in the brain tissue (Figure 1). However, n the brain tissue of the second group mice proliferation of neurocytes, significant edema and dilated vessels were observed (Figure 2).

There was no pathological process in colon tissue of the control group mice. Clearly visible mucosa of the large intestine with small vill, not wide submucosal layer with small vessels were observed (Figure 3).

Histological examination of colon preparations of the experimental group mice showed changes in the intestinal mucosa. There was a focal glandular hyperplasia of the mucosa, up to the development of small polyps (Figure 4). In the mice of this group in the submucosal layer there was edema with an expansion of the submucosa and an increase in the number of small vesicles in this zone (Figure 5).

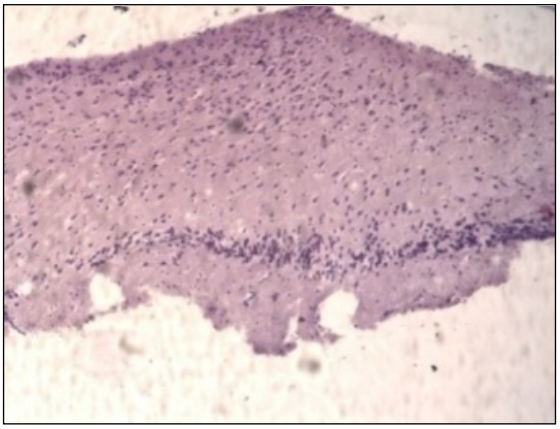

Figure 1. Brain tissue of the control group mice stained with hematoxylin-eosin

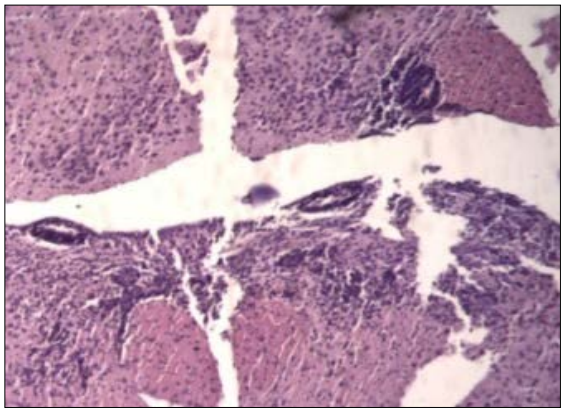

Figure 2. Brain tissue of mice of the second group stained with haematoxylin – eosin.

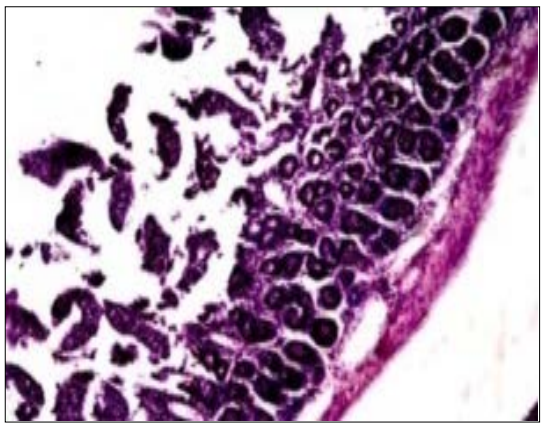

Figure 3. Colon tissue of the control group mice stained with hematoxylin-eosin.

Considering the morphohistochemical picture, the question naturally arises as to how closely the brain and intestinal microbiota are interrelated and what are the main components in this interaction. Intestinal nervous system is represented by two populations of cells, neurons and intestinal glial cells (IGC), which four times exceed the number of neurons. IGC provides several aspects of bowel functioning including peristalsis, micro vascular circulation, secretion of fluid, ions and biologically active peptides, and barrier function. IGC is morphologically and functionally similar to the astrocyte of the central nervous system. It is a key regulator of intestinal homeostasis and an active participant in the development of intestinal pathology.

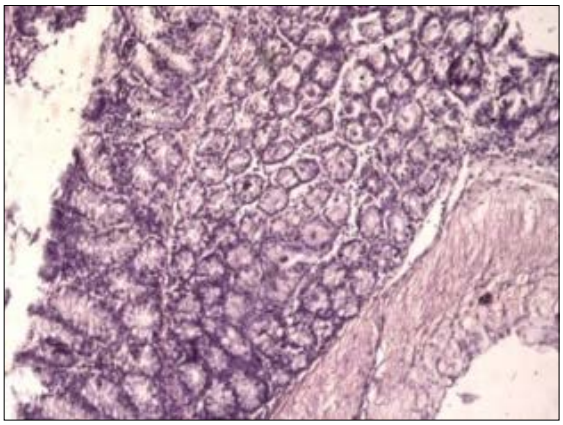

Figure 4. Large intestine of the experimental group mice stained with haematoxylin - eosin.

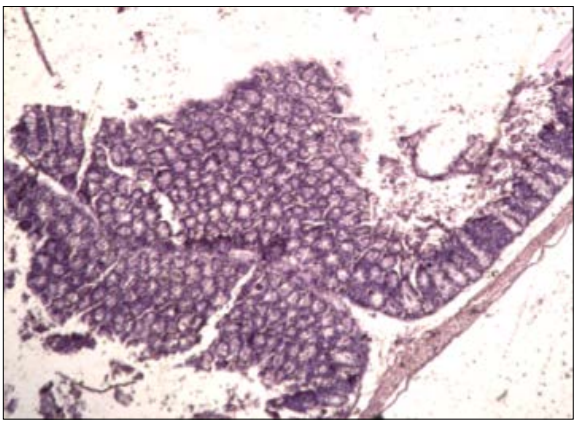

Figure 5. Submucosal layer of the experimental group mice, with hematoxylin-eosin.

A new concept in gastroenterology is that a wide range of diseases associated with impaired peristalsis, including IBD (inflammatory bowel disease), can be diagnosed as intestinal neuropathy. It is still unclear whether neuropathy is a consequence of the disease or its cause. Given the similarity of intestinal glia and astroglion of the brain, the concept deserves special attention. It is the concept of unified mechanisms of intestinal and blood-brain barrier regulation.[16] Glial cells of the intestine are morphologically, immunohistochemically and functionally equivalent to astrocytes of the central nervous system. Intestinal flora affects the sensory, motor and immune functions of the intestine and also interacts with higher nervous centres.

The purpose of this study is to identify some opportunistic microbes, in particular *E. coli*, the pro-inflammatory *St. aureus*, and the associated fungi of the genus *Candida* in dextran sulphate induced non specific ulcerative colitis. Increasing the concentration of microbial toxins contributes to the development of a variety of pathological processes in the human body. It is shown that thermolabile enterotoxins of various conditionally pathogenic enterobacteria, including *E. coli*, cause an increase in the permeability of the mucous membranes of the gastrointestinal tract. Changes in the appearance and behaviour of the animals viz., a depleted species, a discharge of blood from the perianal region, thin and cyanic peritoneum of the mice was observed as a result of the experiments.[17] On sowing in nutrient broths and subsequent re-crossings on solid nutrient media single colonies of *E. coli* were isolated from brain washings. Similarly, *St. aureus* and hemolytic *E. coli* were separated from the cultures of the contents of the large intestine. Coliforms were not found in the blood, so the phenomenon of translocation of microbes is ruled out. Ample growth of *St. aureus*, that resembled sepsis, was revealed following the studies in the blood. Fungi of the genus *Candida* were also observed in significant numbers throughout the all samples

The barrier function of the epithelium is the key in the development of inflammatory bowel diseases. While the normal functioning requires a constant balance between reactivity and tolerance to the microorganisms of the intestinal lumen, increased permeability of the intestinal mucosa is the main risk factor for the spread of bacteria. Epithelium being an important element of tissue barriers provides selective transport for the movement of ions and macromolecules, and also creates an obstacle for their penetration into the underlying tissues. The permeability of the epithelial layer is controlled by the apicalinter cellular complex - dense contacts, consisting of proteins of the claudine family.[18] In acute inflammatory processes such as NUC caused by DSS, conditionally pathogens and pathogenic microorganisms, colonizing the small intestine mucous surfaces, forming bioplasts and can become a source of bacterial toxin. When the epithelial layer breaks they penetrate into the lymphatic and circulatory system and cause sepsis.

A two-week treatment of the mice with the mixture of probiotics, in free and immobilized forms, following DSS induced non specific ulcerative colitis (DSS-NUC), indicated that both probiotics and PBZ completely normalized microbiota in 14 days. The probiotics used in our studies contribute to the restoration of the intestinal microbiota, in particular by a sharp decrease in the number of fungi of the genus *C. albicans*, which resulted from a sharp drop in the body's immune status. In mice with NUC, probiotics destroy pro-inflammatory staphylococcus and restores the proportion of *E. coli*, which appropriately correlates with the intestinal microbiom preventing the further development of sepsis.

Acute colitis manifested as diarrhea and bloody feces, in some cases rectal prolapsed, has occurred as a complication in colitis models using sodium dextran sulphate.[19] PBZ shortened the duration of diarrhea in one day, whereas it was lasted longer, approximately for 1-2 and 2-3 days, during treatment with probiotics. This is presumably, because of a species-specific efficacy of probiotics in the treatment of acute diarrhea, and *L. rhamnosus* included in the probiotics mixture is the effective one.[20] Body weight of animals (29.67 ± 1.97 g) decreased during sodium dextran sulphate-induction of nonspecific ulcerative colitis up to 13.5 - 16.9 % at the end of DSS administration, and began to reverse by10 days post-DSS and tendency to gain normal weight was observed until mice were sacrificed on day 14 post-DSS. Thus, all the tested probiotics prevented diarrhea and bleeding in one-two days, as well as efficiently restored the weight gain suppressed during nonspecific ulcerative colitis that agrees with findings of the other authors.[21]

Colon length and disease activity index were also significantly improved suggesting on-going recovery from the disease. On day 14 post-SDS, the colon length of ulcerative colitis mice was (6.2 ± 0.3 cm) shorter than that of control mice (8.9 ± 0.8 cm). Treatment with probiotics attenuated colon shortening about equally (7.13 ± 0.32 cm and 7.41 ± 0.43 cm respectively), while it was normalized by PBZ. The DAI calculated by diarrhea, visible fecal blood weight loss, as well as colon length and macroscopic damage additional indices for colitis (see Material and methods) reached up to 8-11 in the DSS-treated group, it was significantly lowered to about one-third in the self healing processes on day 14 post-DSS, when all three treatment groups showed complete recovery. The above mentioned parameters correlated with histological grading of colitis based on the amount and depth of inflammation, as well as the amount of crypt damage or regeneration, and the percentage involvement by the disease process.

Histopathological changes observed in the colon and brain regions of corticolimbic system were examined using H&E staining. As in many other findings microscopic features of sodium dextran sulphate-induced nonspecific ulcerative colitis was characterized by epithelial damage, disruption of crypt architecture, and inflammation.[22] Inflammatory cell infiltration in the areas of focal lesions, and edema in the colonic submucosal layer were detected (Figure 6 A, B and C).

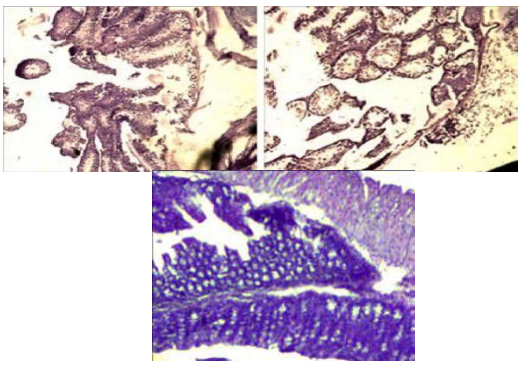

Figure 6. Histopathological changes in the mouse colon following sodium dextran sulphate-induced nonspecific ulcerative colitis (upper row) and 14 days post-colitis (lower row). Erosions in the colonic mucosa, edema and inflammation in the subepithelial layer (A, B) x100. The intestinal wall with the mucous glandular hyperplasia and formation of the hyperplastic polyp (C) x100.

It should be noted that acute inflammatory or infectious process are accompanied by vasodilatation with increased capillary permeability and extravasation of protein-aqueous fluid in a loosely packed submucosal layer resulted in the edema relative to a thickened echogenic submucosal layer, there to mucosal hyperplasia seen in nonspecific ulcerative colitis mice is an initial step in the formation of polyps, which were also found, indicating an acute disease process.[23]

Two weeks after stopping sodium dextran sulphate, the recovery phase of sodium dextran sulphate-induced nonspecific ulcerative colitis was associated with epithelial apoptosis and disruption of the mucosa, the submucosa contained some macrophages, and lymphoid micro follicles were seen in lamina propria, as well as the colonic epithelial cell proliferation that involved in the regeneration processes.[24] However, in some places edema and erosions and focal glandular hyperplasia in the colonic mucosa were observed, epithelium was incompletely regenerated (Figure 7 D, E and F).

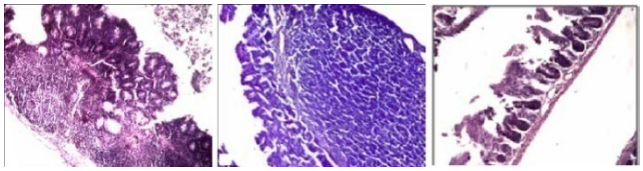

Figure 7. Histopathological changes in the mouse colon following sodium dextran sulphate-induced nonspecific ulcerative colitis (upper row) and 14 days post-colitis (lower row).Focal glandular hyperplasia of the mucosa (D) x100, H&E stain; ero-sions in the colonic mucosa, edema and inflammation in the subepithelial layer (E) x100 H&E stain; intact mouse colonic mucosa with not wide subepithelial layer (F), x100 H&E stain.

It is of interest to note that the sodium dextran sulphate-induced non specific ulcerative colitis caused edema and proliferation of glial cells in the mouse brain tissues lasted for the post-SDS period with manifestation of gangliomatous atypical nervous cells (Figure 8).

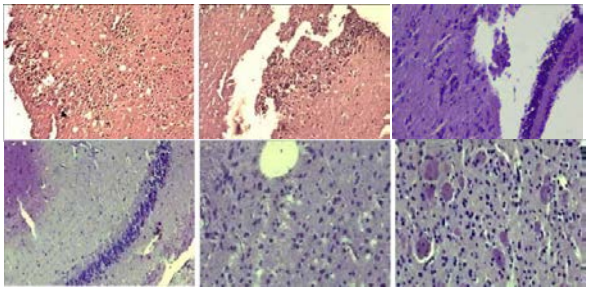

Figure 8. Histopathological changes in the mouse brain following sodium dextran sulphate -induced colitis (upperrow) and 14 days post-colitis (lower row) . Edema and proliferation in the brain tissues (A, B), intensive focal proliferation of glial cells, and edema (D, E), and manifestation of gangliomatous cells (F). (H&E stain,100 X).

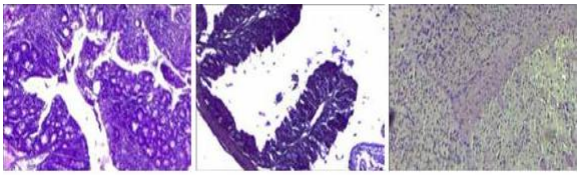

Figure 9. Effect of probiotic-treatment on the histopathological changes in colon and brain following sodium dextran sulphate-induced ulcerative colitis. (A) x 40, H&E stain. (B), x 100, H&E stain (C), x 40, H&E stain.

Probiotics treatment attenuated hyperplastic changes and prevented the polyp formation in the colon though some place mucosal glandular hyperplasia and moderate inflammation were detected (Figure 9 A). Notably, hyperplasia may be due to any number of causes, including chronic inflammatory response, compensation for damage or disease elsewhere.[25] The probiotics-treated mice showed increased crypt height compared to self-healing post-SDS mice (Figure 9 B). Surprisingly, the brain regions of probiotics-treated mice were well preserved and did not undergo deleterious changes observed in both sodium dextran sulphate-induced non-specific ulcerative colitis and post-SDS period (Figure 9 C).

On the preparations of the PBZ-treated mice slight inflammation and proliferation of epithelial cells were observed, and some place deformed crypt structures occurred (Figure 10 A and B).

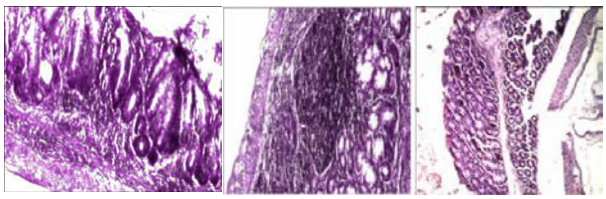

Figure 10. (A) PBZ-treatment presented the colonic wall x 40, H&E stain; the lymphoid macrofollicles in the colonic mucosa (B), x 100 H&E stain and in the subepithelial layer (C) x 100 H&E stain.

However, the layers of the mucosa are preserved, and in the colonic lamina propria the clusters of lymphoid structures are presented both in the form of follicles and in the form of diffusely located lymphoid elements, among which plasma cells and macrophages were found (Figure 10 C). Gut-associated lymphoid tissue is known play a pivotal role in there pair mechanisms. In inflammatory conditions, increased number, diameter and density of isolated lymphoid follicles suggest their involvement in immune surveillance, their presence is also indispensable in normal mucosal regeneration of the colon, as they serve as a regenerative pool of stem cells in case of mucosal damage, and/or contribute to the optimal cytokine milieu for the differentiation of immigrating stem cells reviewed elsewhere.[26]

Beneficial effect of PBZ treatment was found in the brain, where in some areas the ganglion cells surrounding the nerve structures that play a protective role in nervous tissues were detected. At the same time, in the brain of some PBZ-treated mice we observed signs of a negligible dystrophy, and someplace still widened full-blooded vessels pointed to the possibility of development of the per vascular edema that may be involved in the formation of the per vascular exudative cuff, which plays dual role, on one side it can be implicated in disruption of the blood-brain barrier, on the other can be considered as a protective mechanism of strengthening vascular wall from the outside.[27] Notably, the similarity between perivascular spaces in human and rodent brains and their significance as anatomical routes for edema fluid drainage from damaged brain tissues has been demonstrated.[28]

Effect of the selected probiotics on the behavior and mood of mice

Depression-like behavior of mice was observed immediately after sodium dextran sulphate–induced nonspecific ulcerative colitis. Animals displayed a decreased motor activity in the open field mimicking human psychomotor retardation.[29] Another major symptom of depression, detected in the open field and the elevated plus-maze, was a decreased number of rearing relevant to exploratory behavior showing a "refractory loss of interest".[30] Reduced grooming was also observed and reflects decreased self-care and motivation, another trait of depression-like behavior.[31] Nonspecific ulcerative colitis mice exhibited also a decreased number of hanging (a risk-assessment) in the elevated plus-maze. It has been shown that sodium dextran sulphate nonspecific ulcerative colitis modifies the behavioral responses in mice via impact on cerebral expression of stress related neuropeptide systems and level of pro-inflammatory cytokines in the limbic system.[31] We have previously reported that behavior was no longer impacted at 14 days post-SDS in mild-to-moderate ulcerative colitis, but in severe colitis post-SDS non-treated animals still exhibited attenuated levels of depression and anxiety that disappeared completely in all the three groups of treated mice (Table 1, 2). Number of entries into open arms, percentage of open/total arm entries might also be earned to anxiety resembling human anxiety/depression, while number of enclosed arm entries, total number of arm entries and rearing probably related to motor activity.[32]

Table 1. Effect of treatment on the mice behavior in the open field following DSS-NUC.

Groups	Motor activity	Rearing	Gruming	Defecation boli
Control	47.29±5.68	7.18±1.15	4.33±1.56	1.19±0.65
DSS-NUC	15.3±1.4	1.1±0.3	1.03±0.2	0.02±0.02
Post self-recovery	17 ±2.85	1.6±0.8	1.45±0.71	0.69±0.58
Probiotic - treated	50.33±6.34	2.42±1.08	2.75±1.55	0.42±0.52
PBZ treated	64.83±16.7	7.9±2.5	6.08±1.13	0.69±0.93

According to above mentioned, anxiety/depression was for PB> PBZ (44.8, 47.5, and 59.3 % respectively), and motor activity assessed as a sum of variables the OF and the elevated plus-maze was for PBZ > PB (96.06, 80.92, 66.92, respectively).The number of defecation boli of treated mice from post-SDS group was similar to those of from non-treated group in the open field test. Contrary, both treated and non-treated mice from post-SDS groups showed normalized number of boli in the elevated plus-maze test. Thus, hardly to explain psycho-emotional activity of tested animals with respect to this variable, because of its opposite values determined in two tests used.

However, the other variables in both tests suggested the modulatory effects of all the probiotics, and the most beneficial effect of PBZ on motor and psycho-emotional activity of nonspecific ulcerative colitis-mice. This is in line with findings on regulation of emotional behavior by *Lactobacillus* strain in a mouse via the vagus nerve.[33] Correlation between the changes in microbiota and depression has also been shown.[34] As we mentioned above probiotics via correction of microbiota may enhance gut barrier, modulate immune response, as well as prevent gut-brain alterations relevant to mood and emotions. Probiotic bacteria lactobacillus and bifidobacterium attenuate inflammation in DSS-NUC in mice and may be used for induction of remission in nonspecific ulcerative colitis.[35]

Effect of the selected probiotics in free and immobilized forms on the lipid peroxidation processes following DSS-induced nonspecific ulcerative colitis. Maintaining a redox balance is crucial to preserve gut homeostasis. The gut cells respond to commensal microbiota or pathogens with immunetolerance and proinflammatory signals respectively.

Table 2. Effect of treatment on the mice behavior in the elevated plus-maze following DSS-NUC.

Groups	Rearing	Gruming	Hanging over the arms	Defecation boli
Control (healthy)	6.6±1.04	3.62±0.5	4.93±0.88	1.14± 0.34
DSS-NUC	0.18±0.4**	0	0	0
Post self-recovery	2.5±0.76*	0.18±0.4**	0	0
Probiotic - treated	4.0±0.85*	2.67±1.5$^{\#}$	2.75± 1.29$^{\#}$	0.67± 0.49$^{\#}$
PBZ treated	8.91±3.32$^{\#}$	2.83±0.85$^{\#}$	5.66±1.4$^{\#}$	0.59±0.64$^{\#}$

Notes:M ± SD (n=12). # p >0.05, * p<0.05, ** p <0.01, *** p <0.001 (compared to control)

Reactive oxygen species produced by mucosa-resident cells or by newly recruited innate immune cells are essential for antimicrobial responses and regulation of signalling pathways including processes involved in wound healing. Over production of reactive oxygen species due to up-regulation of oxidases or altered mitochondria l function is linked to nonspecific ulcerative colitis, DSS-NUC is also accompanied by stimulation of lipid peroxidation processes i.e., system-wide oxidative stress response. The colonic MDA level was significantly increased in the DSS-NUC group (0.29 ±0.023 nmol MDA/mg protein) compared to control (0.017 ± 0.008 nmol MDA/mg protein) ($p< 0.001$). Colonic MDA content decreased in post-SDS group, remaining 5.6 times higher than control values. Treatment with probiotics reduced it approximately equally by half compared to self-healing processes, while PBZ interfered with suppression of lipid peroxidation in self-recovery group which requires further study.

Notably, probiotics, PBZ practically normalized MDA levels increased by 6 and 2.6 times in the blood leucocyte and plasma following NUC. At the same time, MDA level has increased by 7.5, 2.5, 2.1, and 2.1 times in the prefrontal cortex, striatum, hippocampus and hypothalamus respectively. Two weeks after stopping DSS, it was normalized in the striatum and hippocampus, but was by 3.6 and 1.3 times high in the prefrontal cortex and hypothalamus compared to control. Of interest probiotics normalized the MDA content in prefrontal cortex, and dropped it drastically below the control: PB from 2.5 to 3.5 times in the striatum, hippocampus and hypothalamus respectively). This may cause a decrease in the physiological level of oxidant challenge that is essential for governing life processes through redox signaling.[36] In this respect the antioxidant effect of PBZ is more acceptable.

However, probiotics significantly inhibit lipid peroxidation preventing oxidative damage in the regions of corticolimbic system that may also contribute to their attenuation of histopathological changes in the brain and prevention mood disturbances following DSS-NUC.Immune-inflammatory processes are one of the main causes of destabilization of the barrier function of intestine and brain. Despite the known protective role of intestinal glee in natural immunity, it can be activated by any pro-inflammatory stimulus, acting as an antigen present in cells and provoking the synthesis of a variety of cytokines. Moreover, the intestinal glia expresses iNOS and L-arginine necessary for the synthesis of nitric oxide (NO), which possesses both protective functions against foreign antigens (viruses and bacteria) and pro-inflammatory properties. The protective role of the intestinal nervous system is determined by the ability of glee and neurons to express Toll receptors (TLR) that recognize microbial and viral pathogens. Binding to the receptor initiates the activation of NF-kB and the transcription of the inflammatory response genes responsible for the synthesis of mediators, including cytokines, which ensure the elimination of the infectious agent, and also regulates epithelial proliferation and its permeability. TLR3 and TLR7 recognizing viral RNA and TLR4 recognizing LPS are detected in intestinal fibrillation, dorsal spinal ganglia of mice and in the ganglion of the vagus nerve. Thus, the intestinal nervous system can be directly activated by bacterial and viral components, carrying out the first line of intestinal wall protection and signaling to the brain in the presence of a threat. Deregulation of inflammation leads to hyper production of cytokines, oxygen metabolites and disruption of the barrier function both of the intestine and the brain. This occurs with systemic inflammation, an indicator of which is an increase C-reactive protein in the blood. Systemic inflammation, as a rule, leads to an increase in LPS in the brain, in those areas where the blood-brain barrier is absent, in the ventricular zones and nearby structures rich in vascular plexuses.[37] Circulating LPS first reaches organs lacking a blood-brain barrier and induces transcription of its own CD14 receptor in the parenchymal structures surrounding the ventricles of the brain and then reaches distant brain structures (in the most severe lesion). Chronic endotoxinemia forms a stable inflammatory condition in the circulatory zones of the brain with subsequent destabilization of the blood-brain barrier and the spread of inflammation to other parts of the brain, which results in the development of neuron-degeneration.[38]

CONCLUSION

In conclusion, the selected strains of probiotics with psychological, antifungal activities in free form and immobilized on the micronized zeolite based composition of chemically modified natural minerals may decrease NUC disease activity index score, improve some of the symptoms associated with NUC, effectively restore gut microbiota balance, alleviate symptoms associated with depression/anxiety and histopathological changes in colon and brain, and protect against oxidative stress via inhibition of lipid peroxidation in the colon, blood and regions of corticolimbic system following DSS-NUC.

References

[1]Bondarenko V.M., Ryabichenko, E. V., Intestinal – brain axis. Neuronal and immune-inflammatory and mechanisms of brain and intestinal pathology, *Zh. Microbiol. Epidemiol. Immunobiol*., **2013**(2), 112-120.

[2]Bondarenko, V. M., Lichoded, V. G., Persistence of biologically active components of microflora of the gastrointestinal tract, *Zh. Microbiol. Epidemiol. Immunobiol*., **2012**(4), 82-87.

[3]Buresh, Ya., Bureshova, O., Houston, P., *Techniques and basic experiments on the study of the brain and behaviour*, Elsevier, Amsterdam, **1991,** 399.

[4]Neufeld, K. M., Kang, N., Bienenstock, J., Foster, J. A., Reduced anxiety-like behavior and central neurochemical change in germ-free mice, *Neuro-gastroenterol. Motil*., **2011,** *23*, 255-264. doi: 10.1111/j.1365-2982.2010.01620.x.

[5]Willis, C. L., Glia-induced reversible disruption of blood-brain barrier integrity and neuropathological response of the neurovascular unit, *Toxicol. Pathol.*, **2011,** *39*(*1*), 172–185. DOI 10.1177/0192623310385830

[6]Porfenov, A. I., Bondarenko, V. M., What we gained from acentary of investigation of symbiotic intestinal microflora, *Arch. Pathol.,* **2012,** *2*, 21-25.

[7]Aristovskaya, T. V., Vladimirskaya, M. E., Gollerbach, M. M., Katanskaya, G. A., Kashkin, P. N., (editor Seliber G. L.), *Bolshoi praktikum po mikrobiologi*, Moskva, Vysshaya Shkola, **1962**, 491.

[8]Mery, C., Guerrero, L., Alonso-Gutierrez, J., Figueroa , M., Lema, J. M., Montalvo, S., Mena, C., Borja, R., Evaluation of natural zeolite as microorganism support medium in nitrifying batch reactors: influence of zeolite particle size,. *J Environ Sci. Health A: Toxic. Hazard. Subst. Environ. Eng*., **2012**, *47*(3), 420-427. DOI:10.1080/10934529.2012.646129

[9]Melgar. S., Karlsson, A., Michaëlsson, E., Acute colitis induced by dextran sulfate sodium progresses to chronicity in C57BL/6 but not in BALB/c mice: correlation between symptoms and inflammation, *Am. J. Physiol. Gastrointest. Liver Physiol*, **2005,** *288*(*6*), G1328–G1338. DOI:10.1152/ajpgi.00467.2004

[10]Mitrovic, M., Shahbazian, A., Bock, E., Pabst, M. A., Hol-zer, P., Chemo-nociceptive signalling from the colonis enhanced by mild colitis and blocked by inhibition of transient receptor potential ankyrin 1 channels, *Brit. J. Pharmacol*., **2010,** *160*, 1430-1442.

[11]Brenes Saenz, J. C., Villagra, O. R., Fornaguera Trias, J. ,Factor analysis of Forced Swimming test, Sucrose Preference test and Open Field test on enriched, social and isolated reared rats, *Behav. Brain Res*., **2006,** *169*, 57–65. https://www.sciencedirect.com/science/article/pii/S016643

[12]Pokrovsky, V. I., Guidelines for microbiological diagnosis of enterobacteria-associated diseases (Metodicheskie ukazaniya po mikrobiologicheskoy diagnostike zabolevaniy, vyzyvaemukh enterobakteriyami, MU 04-723/3, Moscow, MH, USSR , **1984** (in Russian).

[13]Dieleman, L. A., Palmen, M. J., Akol, H., Bloemena, E., Pena, A. S., Meuwissen, S. G., Van Rees, E. P., Chronic experimental colitis induced by dextran sulphate sodium (DSS) is characterized by Th1 and Th2 cytokines, *Clin. Exp. Immunol*., **1998,** *114*, 385–91. https://www.semanticscholar.org

[14]Vladimirov, Yu. A., Archakov, A. I., *Lipids peroxidation in biological membranes*, Nauka, Moscow, **1972,** 252.

[15]Lowry, O. H., Rosebrough, N. J., Farr, A. L., Randall, R. J., Protein measurement with the Folinphenol reagent, *J. Biol Chem*., **1951,** *193*, 265-275.

http://www.jbc.org/content/193/1/265.long

[16]Savide, T. C., Sotroniew M. V., *Labor. Investig*., **2007**, *87*, 731-736.

[17]Bacsoti, G., Villanacci, V., *Gastroenterology*, **2007**, *18(30)*, 4035-4041.

[18]Sun, Y., Zheng, Y. H., *J. Virology*, **2008**, *82(11)*, 5562-5571.

[19]Byrnes, J. J., Gross, S., Effects of the ACE2 inhibitor GL1001 on acute dextran sodium sulfate-induced colitis in mice, *Inflamm. Res*., **2009,** *58*, 819–827. https://www.researchgate.net/publication/26283348

[20]Mantegazza, C., Molinari, P., D'Auria, E., Sonnino, M., Morelli, L., Zuccotti, G. V., Probiotics and antibiotic associated diarrhea in children: A review and new evidence on Lactobacillus rhamnosus GG during and after antibiotic treatment, *Pharmacol. Res*., **2018,** *128*, 63-72. doi: 10.1016/j.phrs.2017.08.001.

[21]Shi, L. H., Balakrishnan, K., Thiagarajah, K., Mohd. Ismail, N. I., Yin O. S., Beneficial Properties of Probiotics, *Trop. Life Sci. Res*., **2016,** *27*, 73–90.

[22]Aviello, G., Knaus, U. G., ROS in gastrointestinal inflammation: Rescue or Sabotage? *Brit. J. Pharmacol*., **2017**, *174(12)*, 1704-1718.

[23]Sipos, F., Muzes, G., Galamb, O., Spisák, S., Krenács, T., Tóth, K., Tulassay, Z., Molnár, B., Thepossible role of isolated lymphoid follicles in colonic mucosal repair, *Pathol. Oncol. Res*., **2010**, *16(1)*, 11-18. https://doi.org/10.1007/s12253-009-9181-x

[24]Edelblum, K. L., Washington, M. K., Koyama, T., Robine S., Baccarini, M., Polk, D. B., Raf. protects against colitis by promoting mouse colon epithelial cell survival through NF-κB, *Gastroenterology*, **2008**, *135(2)*, 539–551. https://www.gastrojournal.org/article/S0016-5085(08)007

[25]Porth, C. L., *Essentials of Pathophysiology: Concepts of Altered Health States*, Lippincott Williams & Wilkins, Philadelphia, U. S. A., **2011**.

[26]Frisoli, J. K., Desser, T. S., Jeffrey, R. B., Thickened sub-mucosal layer: a sonographic sign of acute gastrointestinal abnormality representing submucosal edema or hemorrhage.2000 ARRS Executive Council Award II. American Roentgen Ray Society, *Am. J. Roentgenol*, **2000**, *175(6)*, 1595-1599.

[27]Semenov, I. V., Theoretical questions of etiology, pathophysiology, pathomorphopia and culturology of spiritual and psychosomatic diseases Edema, violation of the BBB and pathology of the vascular wall, **1984.**

[28]Kida, S., Kato, T., Microendophenotypes of Psychiatric Disorders: Phenotypes of Psychiatric Disorders at the Level of Molecular Dynamics, Synapses, Neurons, and Neural Circuits, *Curr. Mol. Med*., **2015,** *15(2)*, 111-118. http://www.eurekaselect.com/129012

[29]Wilner, P., Validity, reliability and utility of chronic mild stress model of depression: 10-year review and evaluation, *Psychopharmacology*, **1997**, *134*, 319–329

[30]Katz, R. J., Roth, K. A., Carrol, B. J., Acute and chronic stress effects on open field activity in the rat: implications for a model of depression, Neurosci. Biobehav., **1981**, *5(2)*, 247-251. https://www.sciencedirect.com/science/article/pii/0149763

[31]Cruz, A. P. M., Frei, F., Graeff, F. C., Ethopharmacological analysis of rat behavior on the plus-maze, *Pharmacol. Biochem. Behav*., **1994**, *49*, 171–176. https://eurekamag.com/pdf/008/008628931.

[32]Reichmann, F., Hassan, A. M., Farzi, A., Jain, P., Schuligoi , R., Holzer, P., Dextran sulfate sodium-induced colitis alters stress-associated behaviour and neuropeptide gene expression in the amygdala-hippocampus network of mice. *Sci. Rep.*, **2015**, *5*, 9970. https://www.researchgate.net/publication/278301316

[33]Bravo, J. A., Julio-Pieper, M., Forsythe, P., Kunze, W., Dinan, T. G., Bienenstock, J., Cryan, J. F., Inges-tion of Lactobacillus strain regulates emotional behavior and central GABA receptor expres-sion in a mouse via the vagus nerve. *Curr. Opin. Pharmacol*., **2012**, *12 (6)*, 667-672. doi:10.1016/j.coph.2012.09.010.

[34]Naseribafrouei, A., Hestad, K., Avershina, E., Correlation between the human fecal microbiota and depression, *Neurogastroenterol. Motil*., **2014**, *26*, 1155–1162. https://onlinelibrary.wiley.com/doi/abs/10.1111/nmo.12378

[35]Mallon. P., McKay, D., Kirk, S., Probiotics for induction of remission in ulcerative colitis, *Cochrane Database Syst. Rev*., **2007**, *17*, CD005573.

[36]Sies, H., Hydrogen peroxide as a central redox signaling molecule in physiological oxidative stress: Oxidative eustress. Redox Biology, 2017, 11. 613-619. https://doi.org/10.1016/j.redox.2016.12.035

[37]Lee ,K. J., Tack, J., Altered intestinal microbiota in irritable bowel syndrome, *Neurogastroenterol. Motil*., **2010**, *22(5)*, 493-498. https://onlinelibrary.wiley.com/doi/abs/10.1111/j.1365-2982.2010.01482.x

[38]De Legge, M. H., Smoke A., Neurodegeneration and inflammation, *Nutr. Clin. Pract.*, **2008**, *23(1)*, 35-41.

Received: 09.12.2018.
Accepted: 03.03.2019.